"Profile Method" for the Measurement of k L a and k V a in Distillation Columns. Validation of Rate-Based Distillation Models Using Concentration Profiles Measured along the Column

ARTICLE *in* INDUSTRIAL & ENGINEERING CHEMISTRY RESEARCH · MAY 2010

Impact Factor: 2.59 · DOI: 10.1021/ie901690m

3 AUTHORS:

Frantisek Rejl
University of Chemistry and Technology, P…
21 PUBLICATIONS **55** CITATIONS
SEE PROFILE

L. Valenz
University of Chemistry and Technology, P…
20 PUBLICATIONS **70** CITATIONS
SEE PROFILE

Vaclav Linek
University of Chemistry and Technology, P…
93 PUBLICATIONS **1,484** CITATIONS
SEE PROFILE

"Profile Method" for the Measurement of k_La and k_Va in Distillation Columns. Validation of Rate-Based Distillation Models Using Concentration Profiles Measured along the Column

F. J. Rejl, L. Valenz, and V. Linek*

Department of Chemical Engineering, Prague Institute of Chemical Technology, CZ-166 28 Prague 6, Czech Republic

The "profile method" enables the determination of vapor- and liquid-side volumetric mass-transfer coefficients k_Va and k_La by comparing the concentration profiles measured in both phases in a distillation column with the simulated profiles. The method is based on the fact that the shape of the concentration profiles along the column depend significantly on the distribution of the mass-transfer resistance between the liquid and vapor phases. This makes it possible to measure k_La and k_Va directly in the distillation columns, in the same manner that is possible in absorption columns, and therefore to validate the distillation models more conclusively than by means of comparing the experimental and calculated height equivalent to a theoretical plate values. The coefficients were measured on structured packing Mellapak250Y. A small axial mixing of phases on this type of packing enables the use of a plug-flow model for both phases. Three distillation systems, methanol−ethanol, ethanol−propanol, and methanol−propanol, were used under total reflux and atmospheric pressure. Samples of the phases were withdrawn directly from the column packing by means of special sampling devices. The dependence of the individual transport coefficients on the phase flow rate was obtained by changing the reboiler duty. The dependencies were compared with those predicted by the following three mass-transfer correlations developed for packed columns: RBF (Rocha et al. *Ind. Eng. Chem. Res.* **1996**, *35*, 1660), BS (Billet, R.; Schultes, M. *Trans. Inst. Chem. Eng.* **1999**, *77*, 498), and DELFT (Olujic et al. *Chem. Eng. Proc.* **1999**, *38*, 683). The coefficients obtained by the profile method differ substantially from those calculated from the original models. Specifically, all of the original models considerably overvalue the k_La coefficients (RBF by up to 2 times, BS by up to 1.5 times, and DELFT by up to 6.3 times) and undervalue the k_Va coefficients (all by up to 2 times). The dependence of the mass-transfer coefficients on the rate of the phases predicted by any of the original models is not consistent with that of the profile method. It has also been shown that the experimental concentration profiles strongly differ from the profiles calculated from the Aspen Plus simulation program. The correlations of the k_La and k_Va coefficients with improved flow dependencies according to the profile method are presented. The concentration profiles calculated from the improved correlations fit the profiles accurately.

1. Introduction

1.1. Transport Parameters in Rate-Based Models of a Packed Distillation Column. Many correlations have been published for the calculation of the partial transport coefficients k_L and k_V and the effective mass-transfer area a on random and structured packing. Wang et al.[1] reviewed the correlations developed during the last decades, from among which we employ in this work the models presented by Rocha et al.[2,3] (RBF), Billet and Schultes[4] (BS), and Olujic et al.[5] (DELFT). The forms of the correlations are derived from simple hydrodynamic and transfer models, which are then designed or rectified, according to the results of the absorption experiments, which enable the measurement of these transport coefficients separately. Validation of these relations has hitherto been carried out by comparing the predicted height equivalent to a theoretical plate (HETP) values with the experimental values established by the product concentrations.

Taylor[6] gave a telling assessment of the present state-of-the-art in distillation model validation with the following conclusion: "To properly validate *any* column model (be it EQ with efficiencies, NEQ, or CFD), it is necessary to measure composition profiles along the flow path(s)—not at all an easy task (especially for packed columns). Such data are, however, essential. Product concentrations are useless for evaluating column models, as almost any model, sometimes even relatively simple black boxes, can be validated with such data. Measured composition profiles, especially in reactive and three-phase distillation processes, would be especially welcome, much more so than more profiles computed from increasingly sophisticated models."

Validation of the models by means of the product concentrations has led to situations in which the resulting HETP values, predicted by various models, agree well with the experimental data, despite the fact that the values of the transport parameters differ by multiples. An example is shown in Table 1: The models predict an almost identical value of HETP = 0.31 m for atmospheric rectification of the methanol−propanol (M−P) mixture. Nevertheless, the DELFT model presumes a k_La value of double and a k_Va value of half in comparison with the RBF model, and the BS model presumes an a value of half in comparison with the RBF and DELFT models. This indicates an unsatisfactory relevance of the parameters used in the simulation models of the processes occurring in distillation

Table 1. Transport Data of M−P ($x_A = 0.0782$; $P = 40$ kW)

model	k_La, s^{-1}	k_Va, s^{-1}	a, m^{-1}	HETP, m
RBF	0.0322	7.91	208	0.313
BS	0.0303	9.55	106	0.304
DELFT	0.0755	4.34	235	0.311

* To whom correspondence should be addressed. E-mail: linekv@vscht.cz.

10.1021/ie901690m
Published on Web 03/26/2010

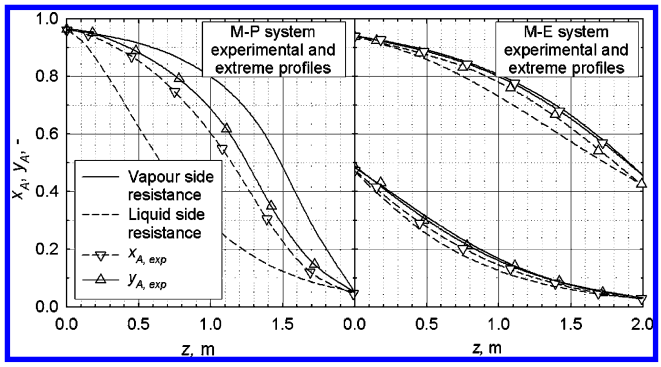

Figure 1. Comparison of concentration profiles calculated, provided the mass-transfer resistance is concentrated in the liquid or vapor phase, with the experimental profiles measured at identical product concentrations.

columns and their degradation into purely matching parameters with no clear physical meaning. However, the clear physical meaning of these parameters underlies their applicability for other distillation systems and the loadings of the column and condition their transferability to similar processes like absorption.

The aim of this work is to determine the $k_L a$ and $k_V a$ in the distillation column by the profile method[7,8] applied to experimental data measured on the structured packing Mellapak250Y. A small axial mixing of phases on this often used packing makes it attractive for the profile method because the results are less biased by the hydrodynamic plug-flow model utilized. The values of $k_L a$ and $k_V a$ and their dependence on the rate of phases are then utilized for qualitatively higher validation of the models presently in use for the calculation of these parameters in the rate-based models of distillation.

1.2. "Profile Method" Measurement of Volumetric Vapor and Liquid Mass-Transfer Coefficients in a Distillation Column. The effect of the resistance in individual phases on the local mass-transfer intensity changes significantly along the distillation column depending on the local slope of the equilibrium curve, as results from eq 1 for the overall mass-transfer coefficient

$$\frac{1}{K_L a} = \frac{1}{m_A k_V a} + \frac{1}{k_L a} \quad \text{or} \quad R_{total} = R_{vapor} + R_{liquid} \qquad (1)$$

where m_A is the local slope of the equilibrium curve. As a result, the hypothetical concentration profiles in the column differ considerably, when calculated as providing the resistance against the interfacial mass transfer, which is concentrated in the vapor or liquid phase. This is demonstrated in Figure 1, where the hypothetical profiles are compared with the experimental data measured at identical product concentrations. The experimental profile lies between the hypothetical extremes.

The profile method applies the fact that the relative resistance of the individual phases varies along the column, according to eq 1, for the separate determination of the volumetric mass-transfer coefficients in the vapor and liquid phases. Simulated concentration profiles are calculated by integration of the rate-based model, with $k_L a$ and $k_V a$ as the matching parameters. The profile method modifies the values of $k_L a$ and $k_V a$, calculated from the original model RBF, BS, or DELFT, by multiplication with the correction factors b_L and b_V to fit the experimental profiles. The best fit with the experimental profiles is obtained with the optimal values of the pair (b_L, b_V), which is unambiguous. The data obtained from these three different models by the profile method provide similar values of the volumetric mass-transfer coefficient. This supports the premise that the $k_L a$ and $k_V a$ data obtained by the profile method are unique.

2. Mass-Transfer Parameter (k_L, k_V, and a) Correlations Used in This Work

2.1. RBF Model. The Rocha et al.[2,3] relation for the liquid-side mass-transfer coefficient is based on the penetration theory, with the contact time expressed in terms of the average liquid velocity u_{LE} in an actual liquid-phase-flow cross section and a characteristic length, which is identified with the corrugation length d_s of the packing. The resulting value is reduced by a factor of 0.9

$$k_L = 2\sqrt{\frac{0.9 D_L u_{LE}}{\pi d_s}} \qquad (2)$$

The liquid velocity is given by

$$u_{LE} = \frac{u_L}{\varepsilon h_{LR} \sin \alpha} \qquad (3)$$

and h_{LR} is the total liquid holdup given by eq 19 in ref 3.

The relation for the vapor-side mass-transfer coefficient is based on earlier investigations on absorption in a wetted-wall column

$$k_V = 0.054 \frac{D_V}{d_s}\left[\frac{(u_{VE} + u_{LE})\rho_V d_s}{\mu_V}\right]^{0.8} Sc_V{}^{0.33} \qquad (4)$$

u_{VE} denotes the average gas velocity in an actual gas-phase-flow cross section

$$u_{VE} = \frac{u_V}{\varepsilon(1 - h_{LR}) \sin \alpha} \qquad (5)$$

For calculation of the effective mass-transfer area below the loading point, the authors start from the Shi and Mersmann[9] correlation and suggest the following relation:

$$a = a_p F_{SE} \frac{29.12\left(\frac{u_L{}^2 \rho_L d_s}{\sigma}\frac{u_L{}^2}{d_s g}\right)^{0.15} d_s{}^{0.359}}{\left(\frac{u_L \rho_L d_s}{\mu_L}\right)^{0.2} \varepsilon^{0.6}(1 - 0.93 \cos \gamma)(\sin \alpha)^{0.3}} \qquad (6)$$

For sheet-metal packing, they give $\cos \gamma = 0.9$ for $\sigma < 0.055$ N m^{-1}. This is the case for the alcohol systems used in this work.

2.2. BS Model. The Billet and Schultes[4] relation for the liquid-side mass-transfer coefficient is also based on the penetration theory, but the contact time is expressed in terms of the superficial liquid velocity u_L and the mixing length is defined as the equivalent hydraulic diameter d_h of a channel in the packing fully filled with liquid. The resulting value is multiplied by a constant C_L, specific for each type of packing

$$k_L = C_L 12^{1/6} \sqrt{\frac{u_L D_L}{h_{LB} d_h}} \qquad (7)$$

$$d_h = \frac{4\varepsilon}{a_p} \qquad (8)$$

h_{LB} is the total holdup given by eqs 11 and 12 in ref 4.

For calculation of the vapor-side mass-transfer coefficient, the dependence on diffusivity, based on a penetration model in a laminar film from the hindered side, is used and the dependence on the vapor flow rate is deduced from experimental

data. The resulting value is multiplied by a constant C_V, specific for each type of packing.

$$k_V = C_V \frac{a_p^{1/2} D_V}{\sqrt{d_h(\varepsilon - h_{LB})}} \left(\frac{u_V \rho_V}{a_p \mu_V}\right)^{3/4} Sc_V^{1/3} \quad (9)$$

The effective mass-transfer area below the loading point is calculated from the following relation:

$$a = \frac{1.5 a_p}{\sqrt{d_h a_p}} \left(\frac{u_L d_h \rho_L}{\mu_L}\right)^{0.2} \left(\frac{u_L^2 \rho_L d_h}{\sigma}\right)^{0.75} \left(\frac{u_L^2}{d_h g}\right)^{-0.45} \quad (10)$$

It was shown that, below a lower limit for the surface tension of 30 mN m^{-1}, the surface of metals, plastics, or ceramic is completely wetted. If a real liquid has a surface tension below this value (as it is in our case; see Table 3), the calculations have to be performed with the limiting value of 30 mN m^{-1}.

2.3. DELFT Model. The Olujic et al.[5] relation for the liquid-side mass-transfer coefficient is also based on the penetration theory, with the contact time expressed in terms of the effective liquid velocity and the mixing length

$$k_L = 2\sqrt{\frac{D_L u_{LE}}{0.9\pi d_{hV}}} \quad (11)$$

The liquid-phase interfacial velocity u_{LE} is defined by eq 3 in which the total liquid holdup h_{LR} is calculated from eq 11 in ref 5 and the hydraulic diameter d_{hV} of the triangular channel is given as

$$d_{hV} = \frac{\frac{(bh - 2\delta d_s)^2}{bh}}{\left[\left(\frac{bh - 2\delta d_s}{2h}\right)^2 + \left(\frac{bh - 2\delta d_s}{b}\right)^2\right]^{0.5} + \frac{bh - 2\delta d_s}{2h}} \quad (12)$$

The thickness of the liquid film δ is calculated from following relation:

$$\delta = \left(\frac{3\mu_L u_L}{\rho_L g a_p \sin\alpha}\right)^{1/3} \quad (13)$$

It is assumed in this model that the liquid-side mass-transfer coefficient k_L does not depend on the vapor-phase velocity up to the loading point.

The vapor-side mass-transfer coefficients were calculated assuming that the transitional phase flow and, by analogy with heat transfer the overall coefficient, was a geometric mean of the coefficients calculated in the laminar and turbulent regimes, respectively.

$$k_V = \sqrt{k_{V,lam}^2 + k_{V,turb}^2} \quad (14)$$

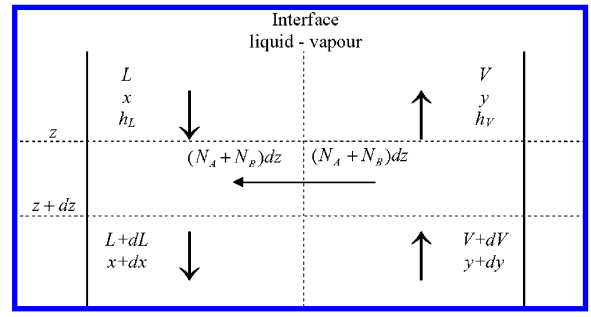

Figure 2. Differential control volume of a distillation column.

where

$$k_{V,i} = \frac{Sh_{V,i} D_V}{d_{hV}} \quad i = \text{lam or turb} \quad (15)$$

$$Sh_{V,lam} = 0.664 Sc_V^{1/3} \sqrt{Re_{Vrv} \frac{d_{hV}}{l_{V,pe}}} \quad (16)$$

$$Sh_{V,turb} = \frac{(Re_{Vrv} Sc_V \xi_{VL} \phi/8)[1 + (d_{hV}/l_{V,pe})^{2/3}]}{1 + 12.7\sqrt{\xi_{VL}\phi/8}(Sc_V^{2/3} - 1)} \quad (17)$$

$$l_{V,pe} = \frac{h_{pe}}{\sin\alpha}; \quad Re_{Vrv} = \frac{\rho_V (u_{VE} + u_{LE}) d_{hV}}{\mu_V} \quad (18)$$

$$\xi_{VL} = \left\{-2\log\left[\frac{\delta}{\frac{d_{hV}}{3.7}} - \frac{5.02}{Re_{Vrv}}\log\left(\frac{\delta}{\frac{d_{hV}}{3.7}} + \frac{14.5}{Re_{Vrv}}\right)\right]\right\}^{-2} \quad \phi = \frac{2d_s}{b + 2d_s} \quad (19)$$

The vapor-phase interfacial velocity u_{VE} is defined by eq 5.

Calculation of the effective mass-transfer area started from the Onda et al.[10] correlation, which is multiplied by the expression $1 - \Omega$, taking into account the perforation of the structured packing

$$a = a_p(1 - \Omega)\left\{1 - \exp\left[-1.45\left(\frac{0.075}{\sigma}\right)^{0.75}\left(\frac{\rho_L u_L}{a_p \mu_L}\right)^{0.1} \left(\frac{u_L^2 a_p}{g}\right)^{-0.05}\left(\frac{\rho_L u_L^2}{a_p \sigma}\right)^{0.2}\right]\right\} \quad (20)$$

where Ω means the portion of the packing surface occupied by holes. In this work, the decrease of the effective mass-transfer area due to the perforation was not considered, $\Omega = 0$.

3. Theoretical Section

3.1. Distillation-Column Model. The distillation process has been modeled as continuous and one-dimensional. The model has been based on mass and energy balances and the mass-transfer relation to a differential control volume $S\,dz$ of the column (see Figure 2) developed on the basis of the following assumptions: (i) the process is the distillation of a binary mixture under total reflux, i.e., $L = V$ and $x = y$ at one/the same cross section of the column; (ii) the process is adiabatic and steady state; (iii) the overall pressure is constant throughout the column; (iv) there is plug flow in both phases; (v) interfacial mass transport is described using a film model in which the convective flow is taken into account; (vi) the rate of heat transfer is such as to keep the vapor and liquid phases just at their dew point and boiling point, respectively; (vii) there is

thermodynamic equilibrium at the interface. A complete set of corresponding model equations can be found in work by Rejl et al.;[8] the algorithm for their solution can be found in work by Linek et al.[7]

3.2. Method of Concentration Profile Calculation. The concentration profile of the liquid phase $x_A(z)$ along the column has been obtained by means of the simultaneous integration of the differential equations

$$\begin{aligned}\frac{dL}{dz} &= f\left(\frac{dx_A}{dz}, \frac{dh_V}{dz}, \frac{dh_L}{dz}, N_A, N_B, x_A, L, h_V, h_L, k_La, k_Va\right)\\ \frac{dx_A}{dz} &= f\left(\frac{dL}{dz}, \frac{dh_V}{dz}, \frac{dh_L}{dz}, N_A, N_B, x_A, L, h_V, h_L, k_La, k_Va\right)\end{aligned} \quad (21)$$

with the initial conditions

$$\begin{aligned}x_A(z=0) &= x_{A0}\\ L(z=0) &= L_0\end{aligned} \quad (22)$$

The molar flow of the liquid phase at the inlet of the column, L_0, is determined experimentally from the volumetric flow F, concentration $x_{A0,exp}$, and temperature of the reflux. The molar fraction of the more volatile component, x_{A0}, in the liquid-phase inlet of the column either is determined experimentally or is subject to optimization (see further). The molar fluxes transferred per unit height of packing N_A and N_B were calculated either with convective flow taken into account from the equation

$$\begin{aligned}N_A &= k_V a c_V r \ln\left[\frac{y_{Aw} - r}{x_A - r}\right]S = k_L a c_L r \ln\left[\frac{x_A - r}{x_{Aw} - r}\right]S\\ r &= \frac{N_A}{N_A + N_B}\end{aligned} \quad (23)$$

or by assuming equimolar counterdiffusion (i.e., the convective flow is not taken into account) from the equation

$$N_A = k_L a c_L (x_{Aw} - x_A)S = k_V a c_V (x_A - y_{Aw})S \quad (24)$$

The volumetric mass-transfer coefficients k_La and k_Va are not considered constant along the column. Their dependence on phase flows and physicochemical properties has therefore been left in the form assumed by the RBF, BS, or DELFT model, and their variability, required for the purpose of optimization, has been retained by application of the multiplication parameters b_L and b_V

$$\begin{aligned}k_La &= b_L(k_L^{model}a^{model})\\ k_Va &= b_V(k_V^{model}a^{model})\end{aligned} \quad \text{model is RBF, BS or DELFT} \quad (25)$$

Enthalpies were calculated from equations

$$\begin{aligned}h_L(x_A, t_L) &= [c_{pLA}x_A + c_{pLB}(1 - x_A)]t_L +\\ \Delta h_{mix}h_V(x_A, t_V) &= [c_{pLA}t_{bpA} + \Delta h_{vapA}]x_A +\\ [c_{pLB}t_{bpB} + \Delta h_{vapB}](1 - x_A) &+ c_{pVA}x_A(t_V - t_{bpA}) +\\ c_{pVB}(1 - x_A)(t_V - t_{bpB})\end{aligned} \quad (26)$$

and their derivatives

$$\begin{aligned}\frac{dh_L}{dz} &= \left[\left(\frac{\partial h_L}{\partial x_A}\right)_{t_L} + \left(\frac{\partial h_L}{\partial t_L}\right)_{x_A}\frac{dt_L}{dx_A}\right]\frac{dx_A}{dz}\\ \frac{dh_V}{dz} &= \left[\left(\frac{\partial h_V}{\partial x_A}\right)_{t_V} + \left(\frac{\partial h_V}{\partial t_V}\right)_{x_A}\frac{dt_V}{dx_A}\right]\frac{dx_A}{dz}\end{aligned} \quad (27)$$

were obtained numerically using dt_L/dx_A and dt_V/dx_A from the dependence of the boiling and dew points on the concentration of the mixture, respectively.

In the calculation, the thermodynamic properties ρ_L, ρ_V, c_{pL}, c_{pV}, Δh_{mix}, Δh_{vap}, σ, μ_L, μ_V, D_L, and D_V were considered as functions of the concentration and temperature, and hence they vary along the column. The corresponding functions were taken from the literature: the molar densities of the liquid mixtures according to Barner-Quinlan's rule, using data from Vargaftik;[11] the vapor phase was considered as ideal, molar heats according to Zábranský et al.;[12] heats of mixing were not considered because the enthalpy change of the liquid phases along the column is 400 times greater than the enthalpy change due to the heat of mixing; the molar heat of vaporization according to Majer and Svoboda,[13] the surface tensions according to Yaws,[14] viscosities according to Reid et al.[15] with the exception of propanol vapor viscosity according to Chung et al.;[16] the vapor−liquid equilibria have been taken from Gmehling et al.[17] and the diffusion coefficients from Zarzycki and Chacuk[18] and those in the liquid using a thermodynamic correcting factor in accordance with Krishna and Wesselingh.[19]

Using the auxiliary relations (23)−(27), the differential equations 21 can be transformed to

$$\begin{aligned}\frac{dL}{dz} &= f(x_A, L; b_L, b_V)\\ \frac{dx_A}{dz} &= f(x_A, L; b_L, b_V)\end{aligned} \quad (21a)$$

The equations, after their replacement with the set of difference equations, have been solved by the Gauss method with b_L and b_V as the sought parameters.

3.3. b_L and b_V Optimization Procedure. Four concentration profiles were calculated according to the procedure described in section 3.2 with estimated values $[b_{L0}, b_{V0}]$ identical for all of these profiles and with the initial conditions $\vec{L}_0$ and $\vec{x}_{A0}$ corresponding with four experimental series, measured at the same reboiler duty. Their mutual consistency was quantified using the objective function

$$\begin{aligned}s &= \sqrt{[\sum_{i=1}^{n}(x_{A,i,cal} - x_{A,i,exp})^2 + \sum_{i=1}^{n}(y_{A,i,cal} - y_{A,i,exp})^2]/2n}\\ x_{A,i,cal} &= y_{A,i,cal}\end{aligned} \quad (28)$$

where s represents the standard deviation of the experimental and calculated molar fractions. The simplex method has been used to search for the optimal pair of parameters $[b_L, b_V]$. Minimization has been performed until the difference in the values of the objective function s in the two following steps was lower than 10^{-7}% of its value and the differences in the parameter values were lower than 10^{-4}% of their values.

In this manner, the profile method provides a set of correction parameters b_L and b_V, which modify values $k_L^{model}a^{model}$ and $k_V^{model}a^{model}$ for the real values in the column according to eq 25, for each of the RBF, BS, and DELFT models and for one reboiler duty. The pairs of parameters b_L and b_V, obtained by minimizing the objective function eq 28, represent the global minimum. This confirmed therefore that the parameters for the different initial estimates $[b_{L0}, b_{V0}]$ do not differ significantly.

4. Experimental Section

4.1. Distillation Column. The experiments were performed in a stainless steel atmospheric distillation column (see Figure 3) with an interior diameter of 0.15 m, packed with 10 pcs of Mellapak250Y, to a height of 2.1 m. Each of the packing pieces was equipped with two wall wipers that redirect the wall flow

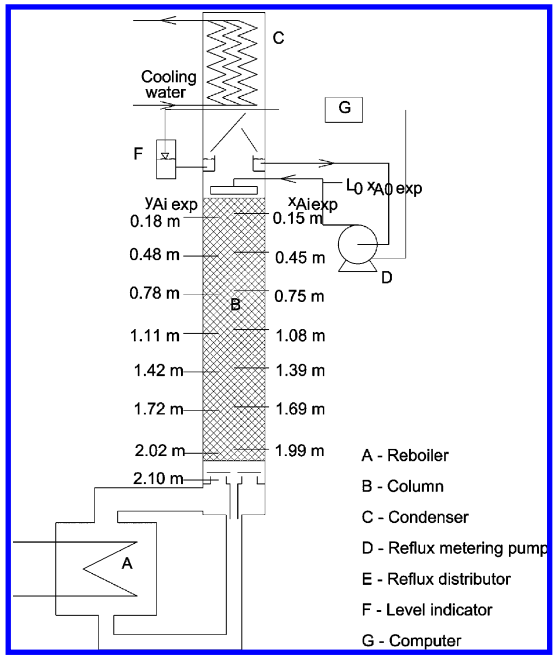

Figure 3. Schematic drawing of the packed distillation column operating under total reflux.

Table 2. Characteristics of Mellapak250Y

a_p (m^{-1})	ε	h (m)	B (m^{-1})	d_s (m)	α (deg)	FSE	Ω	σ_c (N/m)	h_{pe} (m)
250	0.97	0.0117	0.22	0.016 06	45	0.35	0	0.071	0.21

back into the packing. The small diameter of the column and the high number of the wipers justify our assumption that even a small maldistribution of the liquid (higher liquid flow near the column wall) is suppressed substantially in our column. The characteristics of the packing are described in Table 2. An electrically heated reboiler, equipped with an electric power regulator (up to 60 kW), was used to maintain a constant rate of boiling. The power was measured with a three-phase wattmeter (Orbit Merret 405, accuracy 240 W). The complete spiral condenser with a height of 1 m was mounted at the top of the column. The column and reboiler were covered with Orsil insulation. The heat loss, measured by independent experiments, was less than 3% of the reboiler duty.

The column was operated under total reflux, which was maintained by PI regulation of the liquid level in the reflux head. The reflux flow was measured with a radial turbine flowmeter (Omega FTB9510, with an accuracy of 0.001 L min^{-1}). Reflux flow was distributed on the packing using a shower distributor with 25 openings (see Figure 4; 1472 holes m^{-2}). Vapor from the reboiler was introduced into the column by a distributor with four openings regularly spaced over the column base cross section.

The column was equipped with seven openings for the placement of thermistors and sampling devices for the withdrawal of liquid and vapor samples along the column (see Figure 3). A platinum thermometer (Pt 100, accuracy 0.05 °C) was installed in the collecting channel of the sampling device (Figure 5). Note that the sampling tubes were equipped with an overlap, preventing a mixture of the wall-flow liquid with the liquid sampled from the packing. Holes for the sampling devices were drilled through the structured packing with a water jet. We believe the sample points do not affect the phase flow in the packing, notably because the volume of the holes occupies 3.3% of the packing volume only. The column also enables the

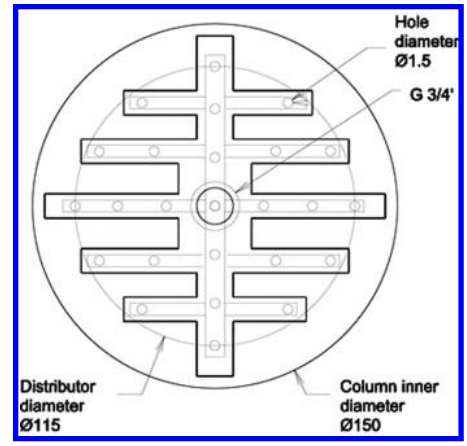

Figure 4. Schematic drawing of the liquid distributor.

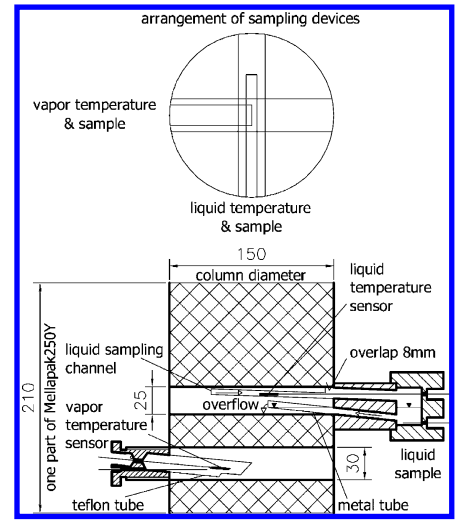

Figure 5. Sampling and measuring device assembly.

withdrawal of samples of the liquid reflux and of the vapor entering the bottom of the column from the reboiler.

4.2. Experimental Procedures, Conditions, and Analytical Methods. Three distillation systems were used: methanol−ethanol (M−E), ethanol−propanol (E−P), and methanol−propanol (M−P). About 45 L of the distillation mixture was poured into the reboiler, and the electric power input to the reboiler was adjusted to the desired level. Four of the power input levels were employed, namely, P = 10, 20, 30, and 40 kW. The column was operated for a sufficient length of time to achieve a steady state, which usually took 1 h. Liquid and vapor samples (2.5 mL) were withdrawn by means of glass syringes from all of the sampling devices simultaneously over a period of approximately 6 min. The vapor phase was withdrawn into a syringe by self-suction due to the self-condensation of vapor inside the syringe, which was cooled by acetone evaporation from the cotton-wool wrapping of the syringe. Analysis of the samples was carried out using a tempered digital refractometer, the Atago RX5000, at 20 °C. The refractometer measures the refractive index with an accuracy of 10^{-5}. The indexes n_D of the pure components of the mixtures differ significantly (n_D: for methanol, 1.32854; ethanol, 1.36123; propanol, 1.38516); the dependence of the mixture indexes on their concentrations does not manifest any extremes, and the accuracy of the molar fraction determination is better than 0.001.

These experiments were repeated four times for every power input with four different concentrations of the mixture in the

Table 3. Vapor and Liquid Flow Rates in the Distillation Column at Limiting Reboiler Duties and Physical Properties of the Distillation Systems Used (p = 101.3 kPa)

	P = 10 kW		P = 40 kW										
x_A	B, m h^{-1}	u_V, m s^{-1}	B, m h^{-1}	u_V, m s^{-1}	t_{bp}, °C	Δh_{vap}, kJ mol^{-1}	$c_L \times 10^{-4}$, mol m^{-3})	c_V, mol m^{-3})	$D_{AB,L} \times 10^9$, m^2 s^{-1}	$D_{AB,V} \times 10^5$, m^2 s^{-1}	$\mu_L \times 10^4$, Pa s	$\mu_V \times 10^4$, Pa s	$s \times 10^3$, N m^{-1}
						Methanol−Ethanol							
0	3.30	0.42	13.2	1.69	78.3	38.6	1.60	34.7	5.28	1.34	4.30	10.4	17.5
0.2	3.14	0.43	12.5	1.70	75.2	38.0	1.71	35.0	5.16	1.35	4.14	10.3	17.8
0.4	2.97	0.43	11.9	1.71	72.2	37.4	1.83	35.3	5.06	1.33	3.96	10.3	18.1
0.6	2.80	0.43	11.2	1.73	69.4	36.8	1.98	35.6	4.97	1.31	3.79	10.2	18.3
0.8	2.63	0.44	10.5	1.74	66.9	36.2	2.14	35.8	4.92	1.27	3.61	10.1	18.6
1	2.45	0.44	9.80	1.76	64.6	35.6	2.34	36.1	4.93	1.25	3.44	10.1	18.8
						Ethanol−Propanol							
0	3.97	0.41	15.9	1.64	97.0	41.9	1.23	32.9	4.13	0.95	4.94	9.59	17.6
0.2	3.81	0.41	15.3	1.64	91.7	41.4	1.29	33.4	3.84	0.93	4.88	9.45	17.7
0.4	3.67	0.41	14.7	1.64	87.4	40.9	1.36	33.8	3.67	0.91	4.76	9.34	17.8
0.6	3.54	0.41	14.2	1.65	83.9	40.2	1.43	34.1	3.61	0.89	4.61	9.24	17.8
0.8	3.42	0.42	13.7	1.67	80.9	39.4	1.51	34.4	3.64	0.88	4.46	9.16	17.7
1	3.30	0.42	13.2	1.69	78.3	38.6	1.60	34.7	3.76	0.87	4.30	9.09	17.5
						Methanol−Propanol							
0	3.97	0.41	15.9	1.64	97.0	41.9	1.23	32.9	4.99	1.24	4.94	9.59	17.6
0.2	3.64	0.41	14.5	1.63	87.6	41.1	1.36	33.8	4.61	1.18	4.74	9.34	18.2
0.4	3.33	0.41	13.3	1.64	79.6	40.0	1.53	34.6	4.39	1.14	4.45	9.13	18.6
0.6	3.03	0.42	12.1	1.66	73.1	38.7	1.74	35.2	4.18	1.10	4.11	8.95	18.9
0.8	2.74	0.43	11.0	1.70	68.0	37.2	1.99	35.7	3.73	1.07	3.77	8.82	19.0
1	2.45	0.44	9.80	1.76	64.6	35.6	2.34	36.1	4.24	1.05	3.44	8.73	18.8

Table 4. b_L and b_V Parameters Calculated with Fixed and Optimized Initial Conditions: System M−P, Model RBF

	fixed initial conditions			optimized initial conditions			
P, kW	b_L	b_V	s	b_L	b_V	s	shift x_A*
10	0.342	3.01	0.0367	0.441	2.11	0.0335	0.0121
20	0.453	1.85	0.0349	0.620	1.32	0.0303	0.0159
30	0.598	1.45	0.0341	0.853	1.08	0.0300	0.0142
40	0.734	1.27	0.0345	1.09	0.993	0.0266	0.0100

* Absolute value of the difference of optimized $x_A(z=0)$ and fixed (measured) $x_{A0,exp}$. Mean values of four series.

reboiler. The concentrations were chosen in order to encompass the entire concentration range of the measured concentration profiles in the column. The result of these experiments is 16 sets of data, each of which includes a set of seven liquid, x_{Ai}, and vapor concentrations, y_{Ai}, along the packing, the liquid concentration in the reflux tube $x_{A0,exp}$, the vapor concentration entering at the base of the column from the reboiler (in the shell of the plate) y_{A8}; the volumetric flow rate of the liquid reflux F, the barometric pressure p, and the average temperature of each phase at the time of withdrawal t_{Li} and t_{Vi}. A complete list of the source data is given in the Appendix. Illustrative vapor and liquid flow rates in the column calculated from the reboiler duties and some physical properties of the distillation systems used are defined in Table 3.

4.3. Data Evaluation Method. Before the final evaluation of all of the experiments, the effect of the three following conditions of the model and their integration with the best-fit parameters b_L and b_V was tested on a narrow set of data: (i) fixed versus optimized initial conditions; (ii) transverse convective flow; (iii) optimization toward the profiles in separate liquid and vapor phases.

(i) Effect of the Fixed or Optimized Initial Conditions in the Search for Parameters b_L and b_V. Within the scope of this test, the parameters b_L and b_V evaluated with the fixed initial conditions $x_A(z=0) = y_A(z=0) = x_{A0,exp}$ were compared with the values evaluated with the initial conditions $x_A(z=0) = y_A(z=0)$ optimized simultaneously in accordance with the parameters b_L and b_V for every set of data measured at the same reboiler duty. The same value of L_0 was used for both initial conditions.

From the results summarized in Table 4, it is apparent that the parameters b_L and b_V evaluated with the fixed and optimized initial conditions differ about 22−49%, but the optimized $x_A(z=0)$ values differ from the measured values $x_{A0,exp}$ just about less than 0.015(!) on average. It is thus evident that the sensitivity of the parameters on the initial conditions is high. Because the optimized values $x_A(z=0)$ did not take any unrealistic values, we have presumed that the optimization of the initial conditions together with the parameters b_L and b_V is a correct method and, hence, this method has been used further.

(ii) Effect of Convective Flow. Convective flow of methanol (A component) $x_A(N_A + N_B)$ induced by the total flow of the mixture through an interface $(N_A + N_B)$ relative to the flow N_A is presented for M−P and M−E distillation systems as a function of the concentration of methanol in Figure 6. The convective flow reaches up to 25% and 12% of the flow of methanol at the top of the column in M−P and M−E systems, respectively, and flows from the liquid into the vapor along the whole column. No reversal of the direction of the convective

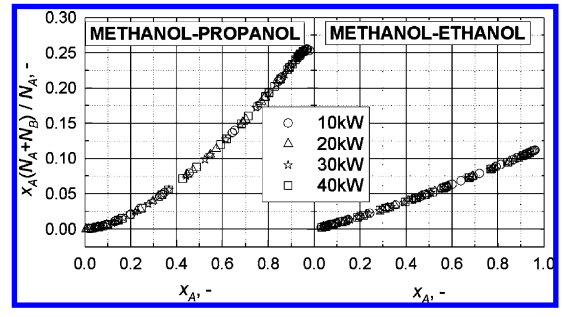

Figure 6. Convective flow of methanol (A component), $x_A(N_A + N_B)$, relative to the flow N_A as a function of the concentration of component A.

Table 5. b_L and b_V Parameters Calculated with (Eq 23) or without (Eq 24) Equimolar Counterdiffusion Considering Convective Flow: System M−P, Model RBF

	With convective flow			equimolar counterdiffusion		
P, kW	b_L	b_V	s	b_L	b_V	s
10	0.449	2.05	0.0335	0.475	2.02	0.0336
20	0.628	1.29	0.0303	0.658	1.28	0.0304
30	0.862	1.06	0.0300	0.907	1.06	0.0301
40	1.098	0.971	0.0266	1.181	0.965	0.0266

flow was observed, in contrast to the system ethanol−water presented in ref 8. An effect of the convective flow on parameters b_L and b_V is, however, minimal. The results presented in Table 5 show that differences of the parameters b_L and b_V evaluated assuming equimolar counterdiffusion, i.e., using eq 24 in the rate-based model of the column, or taking the convective flow into account, i.e., using eq 23, reach 6% at most. Because the calculation with eq 23 does not bring any other problems, except for an increase in the computation time, and is physically more consistent, this model has been used further.

(iii) Effect of Optimization toward the Profiles in the Liquid and Vapor Phases Separately. Experimental liquid and vapor profiles do not coincide with each other (see Figure 7). This is apparently a consequence of the longitudinal mixing of the phases. The plug-flow model was used in both phases of this work in spite of the fact that the model assumes the coincidence of both profiles. The reasons for its application follow. Our hitherto unpublished data[20] concerning the axial dispersion in the absorption tower packed with random (Intalox25) or structured packing (Mellapak250Y) revealed multiple lower longitudinal mixing of the structured packing. Also, the distillation profiles for Mellapak250Y indicate a lesser mutual spacing of vapor and liquid profiles in comparison with the spacing on the random packing (see ref 20). The parameters b_L and b_V, obtained by the adjustment of the liquid concentration profiles and of the vapor profiles, differ only about 10% on average, and the parameters obtained by the adjustment of both of the profiles together constitute roughly their average, as is demonstrated in Table 6. Another reason is that this model has also been used by the authors of mass-transfer correlations, which are compared with the data measured by the profile method in this work.

5. Results

5.1. Temperature of Phases. The liquid phase was found to be overheated at whichever location in the packing for all three distillation systems. This overheating was highest for the M−P system, reaching 3 °C. Vapor was found to be roughly saturated, with the highest deviation from saturation discovered for the M−P system, namely, subcooling by 1 °C. Further analysis of the experimental data achieves these findings: (i) there is no clear relationship between the overheating/subcooling of the phases and the reboiler duty; (ii) the scatter of the overheating/subcooling data is less when it is plotted as a function of the concentration phase than when it is plotted as a function of its position in the column; (iii) subcooling of the vapor phase and overheating of the liquid phase have their maxima at around the equimolar concentration of the mixture, at which the temperature difference of the phases and mass-transfer intensity achieve their maximum values (see the experimental data in Tables A1−A3 in the Appendix).

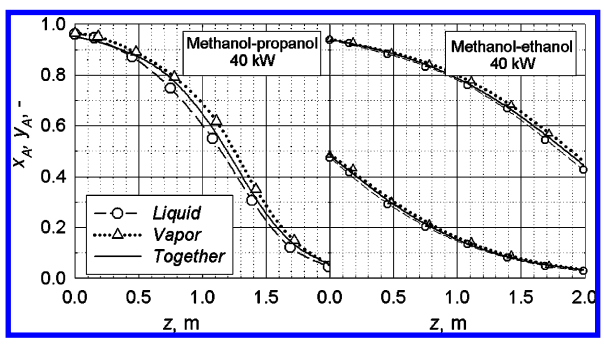

Figure 7. Vapor and liquid concentration profiles adjusted together and separately by the profile method using the RBF model.

5.2. Parameters b_L and b_V and Concentration Profiles Evaluated by the Profile Method. The pairs of the best-fit parameters [b_L, b_V], obtained by minimizing the objective function eq 13, are shown in Table 7, together with the standard deviations s of the experimental and calculated concentrations. The s values show that all of the models with the best-fit parameters obtained by the profile method fit the concentration profiles with practically the same precision. The most precise are the fitted data of the M−E system ($s < 0.018$), and the worst are those of the M−P system ($s < 0.034$). That is why the data for the M−P system are used to illustrate the data behavior obtained by the profile method in the calculations of this work because the deviations for this system are the largest and therefore our conclusions are on the safe side. This is demonstrated clearly in Figure 8, in which the experimental concentration profiles $x_{A,exp}$ and $y_{A,exp}$ are compared with those calculated from the RBF model with the best-fit parameters b_L and b_V for the M−P and E−P distillation systems.

The parameters b_L and b_V depend on the reboiler duty P or, in other words, on the phase flow rates (Table 7). The b_L values increase and the b_V values decrease with P as much as 2-fold in the range of the reboiler duties utilized. This indicates that the individual models do not fit the dependence of the volumetric mass-transfer coefficients on the phase velocities well. This is discussed in section 5.4.

5.3. k_La and k_Va Evaluated according to the Profile Method. The dependence of the volumetric mass-transfer coefficients calculated from the models RBF, BS, and DELFT using the best-fit parameters b_L and b_V on the superficial vapor and liquid phase velocities is shown in Figure 9, together with the coefficients calculated from the original models presented in the literature. The k_Va dependence on the vapor flow rate shows a wide dispersion due to the k_Va dependence on the physical properties of the distillation mixtures, which, not having been eliminated, infiltrates these plots. The differences between the coefficients determined by the profile method and those calculated from the original models can be estimated from the ratio of the corresponding model parameters b. The parameters $b_{L,orig}$ and $b_{V,orig}$ of the original correlations are also give in Table 7. For example, the ratios $b_{L,orig}/b_{L,RBF} = 1/0.474 = 2.11$ and $b_{V,orig}/b_{V,RBF} = 1/2.00 = 0.5$ indicate that the RBF model gives 111% higher k_La and 50% lower k_Va data on average, compared with the profile method in the M−E system at a reboiler duty of 10 kW. From these ratios, it follows that the

Table 6. b_L and b_V Parameters Calculated from Liquid or Vapor and/or Both Concentration Profiles: System M−P, Model RBF

	liquid profile		vapor profile		both profiles	
P, kW	b_L	b_V	b_L	b_V	b_L	b_V
10	0.413	2.27	0.498	1.94	0.449	2.05
20	0.636	1.25	0.595	1.41	0.628	1.29
30	0.825	1.04	0.851	1.13	0.862	1.06
40	1.020	0.990	1.193	0.969	1.098	0.971

Table 7. Best-Fit Parameters b_L and b_V Obtained by the Profile Method

				methanol−ethanol			ethanol−propanol			methanol−propanol		
	$b_{L,orig}$[a]	$b_{V,orig}$[a]	P, kW	b_L	b_V	s	b_L	b_V	s	b_L	b_V	s
RBF	1	1	10	0.474	2.00	0.018	0.418	2.14	0.025	0.449	2.05	0.034
			20	0.564	1.50	0.014	0.580	1.38	0.022	0.628	1.29	0.030
			30	0.763	1.27	0.014	0.794	1.18	0.020	0.861	1.06	0.030
			40	0.971	1.16	0.012	1.025	1.09	0.015	1.098	0.97	0.027
BS[b]	1.334	0.385	10	0.917	0.580	0.018	0.755	0.650	0.025	0.858	0.592	0.034
			20	0.971	0.444	0.014	0.937	0.428	0.022	1.060	0.378	0.030
			30	1.242	0.382	0.014	1.192	0.375	0.020	1.353	0.320	0.030
			40	1.494	0.356	0.012	1.442	0.350	0.015	1.621	0.298	0.027
DELFT	1	1	10	0.196	1.56	0.018	0.158	1.96	0.025	0.178	1.68	0.033
			20	0.259	1.59	0.014	0.249	1.71	0.022	0.289	1.45	0.030
			30	0.392	1.59	0.014	0.369	1.72	0.020	0.447	1.40	0.030
			40	0.534	1.63	0.012	0.493	1.76	0.015	0.596	1.43	0.026

[a] Values of the multiplication parameters used in the original models. [b] Billet and Schultes[4] did not present the constant for Mellapak250Y. For comparison, the constants are presented for similar packing Ralu-Pak.

coefficients predicted by the original RBF model most closely match the coefficients obtained by the profile method at the highest reboiler duty of 40 kW, i.e., at flow rates near the loading point: the differences between k_Va coefficients do not exceed 10% and 16% for k_La coefficients in all of the distillation systems employed. At this reboiler duty, a similar congruence exists between the coefficients calculated from the BS model (the differences do not exceed 22%). In all remaining situations (reboiler duties and distillation systems), all of the original models considerably overvalue the k_La coefficients (by up to 6.3 times; DELFT model) and undervalue the k_Va coefficients (by up to 2 times).

The conclusion is that none of the literature correlations (RBF, BS, or DELFT) describes the distillation mass-transfer coefficients along the column sufficiently accurately for all of the distillation systems used in this work. An encouraging fact is that the volumetric mass-transfer coefficients evaluated from these three different models (RBF, BS, and DELFT), after correction by the profile method, demonstrate mutual compatibility.

5.4. Dependence of k_La and k_Va on Phase Flow Rates. The dependence of the mass-transfer coefficients and interfacial area on the physiochemical properties and on the flow rate of phases allows, to a certain extent, validation of the models for k_La and k_Va evaluation. The physicochemical properties of the alcoholic systems utilized in this work do not vary much. The greatest differences exist between the M−E and E−P systems (see Table 5). The differences in the surface tension and vapor viscosity do not exceed 3% and 10%, respectively, but more noticeable differences occur in the viscosity of the liquid phase (by an average 21%) and in the diffusivity, namely, 34% and 45% on average for the liquid and vapor phases, respectively. The b_L values (see Table 7) evaluated by the profile method in the M−E and E−P systems, utilizing the RBF, BS, and DELFT models, differ on average by about 6%, 7%, and 11%, respectively, for the same reboiler duties, i.e., at the same rate of phases, and similarly the b_V values differ on average by about 7%, 8%, and 12%, respectively. This is why, in this work, the dependence

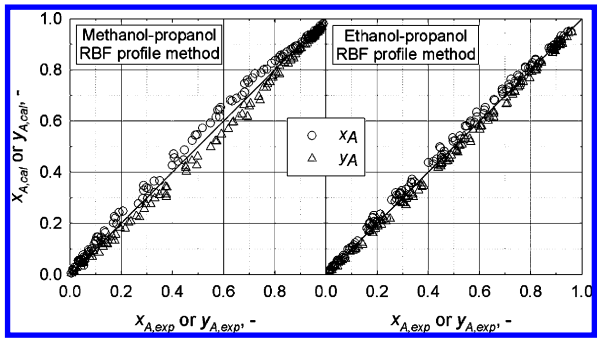

Figure 8. Experimental concentration profiles compared with those calculated from the RBF model with the best-fit parameters b_L and b_V evaluated by the profile method for the M−P and E−P distillation systems.

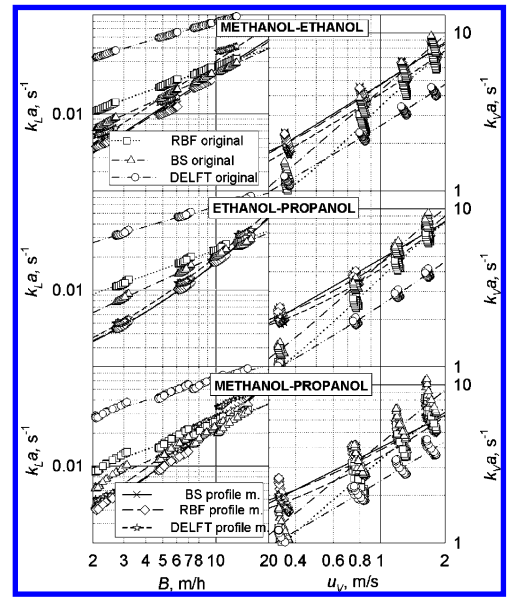

Figure 9. Volumetric mass-transfer coefficients calculated from the models RBF, BS, and DELFT using the best-fit parameters b_L and b_V as a function of the superficial vapor and liquid phase velocities and from the original model correlations.

Table 8. Values of the Exponents in Relations (29) and (33)

	methanol−ethanol			ethanol−propanol			methanol−propanol		
	RBF	BS	DELFT	RBF	BS	DELFT	RBF	BS	DELFT
$\alpha + \varepsilon$	0.597	0.733	0.445	0.596	0.733	0.445	0.597	0.733	0.450
β	−0.015	0	0	−0.020	0	0	−0.017	0	0
ε	0.4	0.4	0.125	0.4	0.4	0.125	0.4	0.4	0.125
$\alpha + \beta + \varepsilon$	0.582	0.733	0.445	0.576	0.733	0.445	0.580	0.733	0.450
λ	0.506	0.339	0.735	0.610	0.432	0.776	0.622	0.437	0.851
$\alpha + \beta + \varepsilon + \lambda$	**1.09**	**1.07**	**1.19**	**1.19**	**1.17**	**1.22**	**1.20**	**1.17**	**1.30**
$\delta + \varepsilon$	0.435	0.408	0.192	0.436	0.408	0.202	0.436	0.408	0.200
γ	0.759	0.750	0.631	0.764	0.750	0.670	0.761	0.750	0.644
$\gamma + \delta + \varepsilon$	1.19	1.16	0.823	1.20	1.16	0.872	1.20	1.16	0.844
υ	−0.350	−0.317	0.025	−0.454	−0.420	−0.078	−0.502	−0.466	−0.111
$\gamma + \delta + \varepsilon + \upsilon$	**0.844**	**0.843**	**0.848**	**0.747**	**0.740**	**0.794**	**0.695**	**0.693**	**0.733**

of the volumetric mass-transfer coefficients on the rate of the phases predicted by the models was tested because it was only possible to change the rates in a wide range, approximately four times, by changing the input into the reboiler.

5.4.1. $k_L a$ and $k_V a$ Dependence on the Rates of Phases Predicted by the RBF, BS, and DELFT Models. It follows from the forms of the correlation that the dependence of the transport characteristics on the rate of the phases can be represented by the following power dependence:

$$k_L \propto u_L^{\alpha};\ k_L \propto u_V^{\beta};\ k_V \propto u_L^{\delta};\ k_V \propto u_V^{\gamma};\ a \propto u_L^{\varepsilon} \qquad (29)$$

We assume that the vapor velocity does not affect the mass-transfer area up to the loading point ($a \propto u_V^0$). Then the dependence of the volumetric coefficients will have the following form:

$$\begin{aligned} k_L a &\propto u_L^{\alpha} u_V^{\beta} u_L^{\varepsilon} \\ k_V a &\propto u_L^{\delta} u_V^{\gamma} u_L^{\varepsilon} \end{aligned} \qquad (30)$$

At total reflux, it holds the following mass balance:

$$u_L S \rho_L = u_V S \rho_V \qquad (31)$$

Relations (30) may therefore be rewritten for the column working under total reflux as follows:

$$\begin{aligned} k_L a &= b_{L,orig} A_L(\text{phys properties})\, u_L^{\alpha+\beta+\varepsilon} \\ k_V a &= b_{V,orig} A_V(\text{phys properties})\, u_V^{\gamma+\delta+\varepsilon} \end{aligned} \qquad (32)$$

$A_{L,V}$ are functions of the physicochemical properties of the system itself that are given by the original models RBF, BS, or DELFT, and $b_{LV,orig}$ are multiplication parameters used in the models that are given in Table 7. The exponents of the power dependence in eq 29, predicted by the RBF, BS, and DELFT models, were obtained by smoothing the data calculated from the respective model within the range of experimental rates (see Table 5) under the following conditions:

$$k \propto u_L^{\chi}|_{u_V=\text{const.}};\ k \propto u_V^{\chi}|_{u_L=\text{const.}};\ u_{L,\text{const.}} = 0.118\ \text{m s}^{-1};\ u_{V,\text{const.}} = 1\ \text{ms}^{-1};\ x_{A,\text{const.}} = 0.5;\ t = t_{\text{boiling}}$$

where k stands for the transport characteristics (k_L, k_V, and a) and χ for the exponents (α, β, γ, δ, and ε). The exponents evaluated are presented in Table 8 for all of the distillation systems.

The overall exponents, $\alpha + \beta + \varepsilon$ and $\gamma + \delta + \varepsilon$, evaluated from the individual models do not depend in practical terms on the rate, concentration, and distillation system within the range of conditions of our experiments. For example, the exponents calculated from the RBF model for the rates $u_L = 0.236$ m s^{-1} and $u_V = 1.8$ m s^{-1} and the system M−P, $\alpha + \beta + \varepsilon = 0.580$ and $\gamma + \delta + \varepsilon = 1.19$, hardly differ from the exponents presented in Table 8 for the half rates, namely, 0.580 and 1.20, respectively.

5.4.2. $k_L a$ and $k_V a$ Dependence on the Rate of Phases Predicted by the Profile Method. When the power input into the reboiler is altered, only the rate of the phases changes significantly in relation to eq 32 (see Table 5). The rate of liquid and vapor in the column rises proportionately to the power. If the $k_L a$ and $k_V a$ dependence on the rate of the phases of the RBF, BS, and DELFT models is described well, the parameters b_L and b_V, obtained by optimization, should not be dependent on the power input to the reboiler. However, the value of the parameter b_L increases with the power for all of the models, and the value of the parameter b_V decreases for the RBF and BS models. This indicates inaccurate $k_L a$ and $k_V a$ dependence on the rate of the phases included in the original RBF, BS, and DELFT models.

The dependence of the experimentally determined parameters b_L and b_V on the power P, i.e., on the mean velocity of the phases in the column, was adjusted in regard to the power relation, in analogy to relations according to eq 29 for the transport coefficients

$$\begin{aligned} b_L &\propto P^{\lambda} \\ b_V &\propto P^{\upsilon} \end{aligned} \qquad (33)$$

The λ and υ exponents found are shown in Table 8. Relations (32) rewritten so as to include the effect of the rate of the phases on the b_L and b_V parameters revealed by the profile method are the following:

$$\begin{aligned} k_L a &= b_{L,profile} A_L(\text{phys properties})\, u_L^{\alpha+\beta+\varepsilon+\lambda} \\ k_V a &= b_{V,profile} A_V(\text{phys properties}) u_V^{\gamma+\delta+\varepsilon+\upsilon} \end{aligned} \qquad (34)$$

Corrected values of the overall exponents $\alpha + \beta + \varepsilon + \lambda$ and $\gamma + \delta + \varepsilon + \upsilon$, presented in Table 8, show that the RBF, BS, and DELFT models considerably undervalue the $k_L a$ dependence on the rate (the exponents in the original models range from 0.445 to 0.733, while the profile method yields values in the range fro 1.06 to 1.37) and considerably overestimate the $k_V a$ dependence (the exponents in the original models range from 1.16 to 1.20, and those in the profile method range from 0.682 to 0.846).

The best-fit parameters $b_{L,profile}$ and $b_{V,profile}$ were obtained by the profile method with the corrected dependence of

Table 9. Best-Fit Parameters $b_{L,profile}$ and $b_{V,profile}$ Obtained by the Profile Method

		methanol−ethanol			ethanol−propanol			methanol−propanol		
	P, kW	$b_{L,profile}$	$b_{V,profile}$	s	$b_{L,profile}$	$b_{V,profile}$	s	$b_{L,profile}$	$b_{V,profile}$	s
RBF	10	17.2	1.35	0.018	30.1	1.42	0.025	36.0	1.35	0.033
	20	13.5	1.24	0.014	25.2	1.31	0.022	30.1	1.24	0.030
	30	14.5	1.27	0.014	26.1	1.36	0.020	30.7	1.27	0.030
	40	15.7	1.35	0.012	27.6	1.45	0.015	32.0	1.35	0.027
BS	10	10.07	0.445	0.018	15.50	0.440	0.025	17.63	0.408	0.033
	20	8.104	0.444	0.014	13.40	0.404	0.022	15.53	0.368	0.030
	30	8.837	0.437	0.014	14.02	0.424	0.020	16.37	0.374	0.030
	40	9.504	0.449	0.012	14.76	0.451	0.015	16.04	0.419	0.026
DELFT	10	36.6	1.72	0.018	36.6	1.94	0.025	72.9	1.65	0.033
	20	26.8	1.72	0.014	30.2	1.79	0.022	59.2	1.51	0.030
	30	29.1	1.67	0.014	31.3	1.84	0.020	61.1	1.51	0.030
	40	31.1	1.69	0.012	32.6	1.92	0.015	62.3	1.59	0.026

Table 10. Mean Values of the Corrected Overall Exponents and the Best-Fit Parameters

	all systems			
	RBF	BS	DELFT	all models
$\alpha+\beta+\varepsilon+\lambda$	1.16 ± 0.050	1.14 ± 0.06	1.24 ± 0.05	1.18 ± 0.066
$\gamma+\delta+\varepsilon+\upsilon$	0.762 ± 0.062	0.759 ± 0.066	0.792 ± 0.047	0.771 ± 0.061
$b_{L,profile}$	24.9 ± 7.4	13.3 ± 3.2	42.5 ± 15	
$b_{V,profile}$	1.33 ± 0.064	0.422 ± 0.027	1.71 ± 0.136	
λ	0.579	0.403	0.787	
υ	−0.435	−0.401	−0.055	

volumetric mass-transfer coefficients on the velocity of the phases using the following relations:

$$\begin{aligned} k_L a &= b_{L,profile} u_L^{\lambda} (k_L^{model} a^{model}) \\ k_V a &= b_{V,profile} u_V^{\upsilon} (k_V^{model} a^{model}) \end{aligned} \quad \text{model is RBF, BS or DELFT} \tag{35}$$

for calculation of the coefficients in optimizing the procedure instead of the relation (25). $b_{L,profile}$ and $b_{V,profile}$ are given in Table 9. The s values, practically the same as those in Table 7, demonstrate that the concentration profiles are fitted with the same accuracy as previously, but the $b_{L,profile}$ and $b_{V,profile}$ values are now practically independent of the phase flow rates and therefore the dependence of the coefficients on the rate is substantively better described.

5.5. $k_L a$ and $k_V a$ Evaluated by the Profile Method with Correction of the Dependence on the Flow Rates of the Phases. The corrected values of the overall exponents $\alpha + \beta + \varepsilon + \lambda$ and $\gamma + \delta + \varepsilon + \upsilon$ presented in Table 8 for different models and distillation systems differ very little from each other. The same holds true for the best-fit parameters $b_{L,profile}$ and $b_{V,profile}$ obtained in different distillation systems. Their mean values are listed in Table 10, together with their standard deviations. Making use of these mean values of the parameters and exponents, the final forms of the mass-transfer correlations referred to in the literature, adjusted according to the profile method, are as follows:

Corrected RBF[2,3] model.

$$\begin{aligned} (k_L a)_{PM,RBF} &= 24.9 {u_L}^{0.579} (k_L a)_{RBF,orig} \\ (k_V a)_{PM,RBF} &= 1.33 {u_V}^{-0.435} (k_V a)_{RBF,orig} \end{aligned} \tag{36}$$

fits the experimental concentration profiles of all distillation systems used with the standard deviation $s_{PM,RBF} = 0.0373$, while the original RBF correlation with $s_{RBF,orig} = 0.121$.

Corrected BS[4] model.

$$\begin{aligned} (k_L a)_{PM,BS} &= 13.3 {u_L}^{0.403} (k_L a)_{BS,orig} \\ (k_V a)_{PM,BS} &= 0.422 {u_V}^{-0.401} (k_V a)_{BS,orig} \end{aligned} \tag{37}$$

fits the profiles with $s_{PM,BS} = 0.0383$, while the original BS correlation with $s_{BS,orig} = 0.0765$.

Corrected DELFT[5] model.

$$\begin{aligned} (k_L a)_{PM,DELFT} &= 42.5 {u_L}^{0.787} (k_L a)_{DELFT,orig} \\ (k_V a)_{PM,DELFT} &= 1.71 {u_V}^{-0.055} (k_V a)_{DELFT,orig} \end{aligned} \tag{38}$$

fits the profiles with $s_{PM,DELFT} = 0.0393$, while the original DELFT correlation with $s_{DELFT,orig} = 0.145$.

Other forms of the correlations may be discussed; e.g., the Reynolds number may be used in place of the velocity. However, such a discussion would perhaps be premature at this time because it is based on a very narrow database of only three distillation systems, with little variance in the physicochemical properties. In this situation, it is difficult to distinguish the exponent values λ and υ, revealed by the profile method, between the exponents of the Reynolds, Weber, and Froude criteria, which include velocity in the original RBF, BS, or DELFT models.

These experimental concentration profiles are compared with those calculated from the corrected RBF model (36) for the M−P and E−P distillation systems in Figure 10. The most accurate are the data of the E−P system and the least accurate those of the M−P system. The standard deviations of the experimental concentrations and those concentrations calculated from eq 36 for the M−E, E−P, and M−P systems are $s = 0.035$, 0.028, and 0.042, respectively. In any case, the correlation (36) is much more precise than the original RBF model with the standard deviations $s = 0.069$, 0.078, and 0.164 for these same systems. Improved accuracy can also be demonstrated for the BS and DELFT models.

The experimental concentration profiles are also compared with those calculated from the *Aspen Plus* simulation program for the M−P and M−E distillation systems in Figure 11 on the log−log scale, which enables detection of the relative differences of the data. In the simulation program, the rate-based model of the distillation columns utilizes either RBF mass-transfer coefficients published by Bravo et al.[22] or BS mass-transfer coefficients published by Billet and Schultes.[23] The profiles

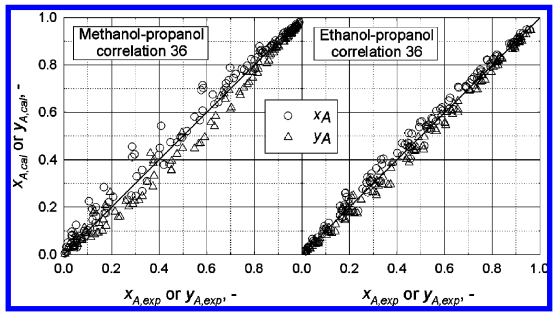

Figure 10. Comparison of the experimental concentrations with those calculated from the corrected RBF model, i.e., from eq 36.

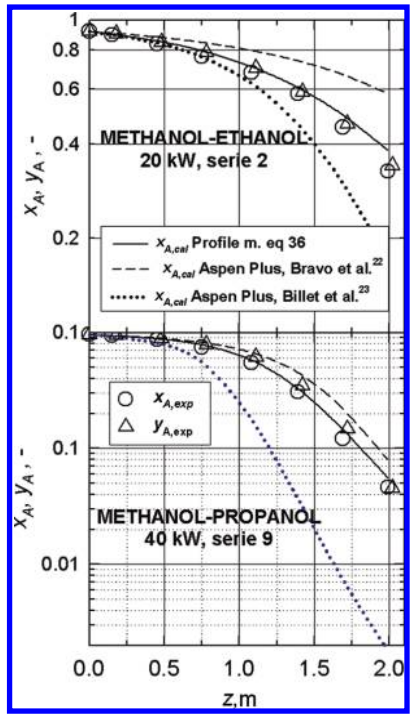

Figure 11. Experimental concentration profiles and profiles calculated from the *Aspen Plus* simulation model and from the profile method correlation (36).

calculated from the profile method correlations (36) and (37) are also plotted in the figure. The product concentrations measured on our distillation column having 5.5 theoretical plates differ considerably from those calculated by the *Aspen Plus* program. The RBF model gives 30% and 70% higher and the BS model (Dr. Schultes informed us that ASPEN has made noticeable mistakes incorporating the BS model into the program simulation and that ASPEN has been informed about these mistakes; unfortunately, it will take some time before corrections will be made) 250 and 1800% lower product concentrations in comparison with the experimental values. The profile method correlations (36) and (37) fit the profiles accurately.

5.6. HETP Values and Relative Liquid-Side Mass-Transfer Resistance. The experimental HETP values were calculated from a number of theoretical plates, as part of the packing, delineated by the liquid concentrations measured at the top and base of the packing part and by the actual height of this part. These are compared with the HETP values evaluated from the concentration profiles calculated by integration of the rate-based model (21), using k_La and k_Va values, calculated from the original RBF, BS, and DELFT models or from their corrected versions, i.e., from eqs 36−38, respectively. The resultant values are plotted in Figure 12 for the M−P and M−E

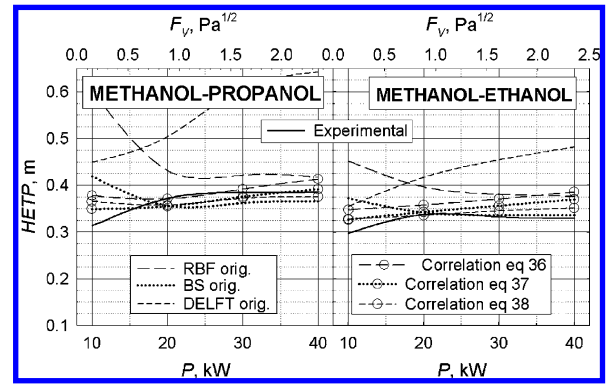

Figure 12. HETP evaluated from the original models RBF, BS, and DELFT or their corrected versions by the profile method, i.e., from eqs 36−38 respectively.

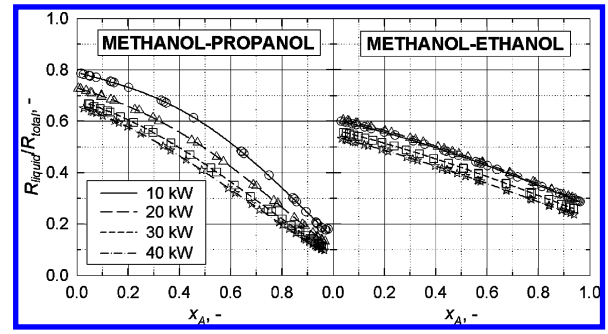

Figure 13. Relative liquid-side mass-transfer resistances calculated from eq 1 using k_La and k_Va obtained by the profile method, using the RBF model with corrected dependence on the velocity of the phases, i.e., with $b_{L,profile}$ and $b_{V,profile}$.

distillation systems. The following conclusions result from the data presented in the figure: (i) HETP values predicted by the original RBF and DELFT models differ considerably from the experimental results; the differences amount to as much as 100%; the original BS model fits the experimental HETP values the best; the maximum difference makes 20% only. (ii) the experimental HETP values are consistent with the values calculated from the three corrected models, RBF, BS, and DELFT, i.e., from the correlations (36), (37), and (38), respectively. (iii) HETP values calculated from these three correlations practically coincide; the differences between them amount to 8% at most.

Variations of the relative liquid-side mass-transfer resistance along the column underlie the applicability of the profile method for the separate evaluation of k_La and k_Va from the concentration profile in the distillation column. The resistance calculated from eq 1 using the mass-transfer coefficients obtained by the profile method, using the RBF model with corrected dependence on the velocity of the phases, is shown in Figure 13. The resistance decreases from the base to the top of the column in all of the distillation systems used and does not manifest any extreme such as, e.g., the ethanol−water system.[8] The greatest change in the resistance occurs in the M−P system at the lowest reboiler duty of 10 kW (from 80% to 20%), and the least change occurs in the M−E system at the highest reboiler duty of 40 kW (from 50% to 10%). In any case, the variation is sufficient for the successful application of the profile method in these distillation systems.

6. Conclusions

The profile method for the simultaneous determination of vapor- and liquid-side volumetric mass-transfer coefficients in

a distillation column was successfully applied on structured packing Mellapak250Y for the atmospheric distillation of three alcoholic systems: M−E, E−P, and M−P. This method calculates the transport coefficients by comparing the concentration profiles measured in both phases with the simulated profiles. The dependence of the coefficients k_La and k_Va on the phase flows and physicochemical properties has been considered in the form assumed in the RBF, BS, or DELFT models, and their variances, which are necessary for the purpose of optimization, have been retained by application of the multiplication parameters b_L and b_V. The choice of the structured packing with minor axial mixing of the phases was driven by the intention to apply a simple plug-flow model for both phases.

It was discovered that the relative liquid-side mass-transfer resistance decreases from the base to the top of the column in all of the distillation systems used and does not manifest any extreme. Variations in the resistance along the column range between 80% and 10% for the M−P system and between 50% and 20% for the M−E system.

The liquid phase along the entire column is overheated for all of the three distillation systems. The highest overheating was registered for the M−P system, reaching 3 °C around the equimolar concentration of the mixture, in which the temperature difference of the phases and mass-transfer intensity achieve maximum values. The vapor phase was more or less saturated.

The convective flow of a more volatile ingredient, methanol, induced by the total flow of the mixture through an interface, reaches up to 25% and 12% of the flow of methanol in the M−P and M−E systems, respectively, but its influence on the parameters b_L and b_V in comparison with their evaluated values, assuming equimolar counterdiffusion, reaches 6% at the most.

The volumetric mass-transfer coefficients obtained by the profile method differ considerably from those calculated from the original RBF, BS, and DELFT models. The original models overvalue the k_La coefficients (by up to 6.3 times; DELFT model) and undervalue the k_Va coefficients (by up to 2 times). The coefficients evaluated by the profile method with these three different RBF, BS, and DELFT models, using the best-fit parameters b_L and b_V, demonstrate mutual compatibility.

The best-fit b_L and b_V parameters depend on the reboiler duty, i.e., on phase flow rates. This indicates that none of the models fits precisely with the dependence of the volumetric mass-transfer coefficients on the phase velocities. According to the profile method, k_La depends on the phase flow in accordance with the relation $k_La \propto u_L^{1.18}$, which is considerably greater than what the original models predict (approximately $k_La \propto u_L^{0.7}$), and k_Va is in accordance with the relation $k_Va \propto u_V^{0.775}$, which is considerably less than what the models predict (approximately $k_Va \propto u_V^{1.2}$). The best-fit parameters $b_{L,profile}$ and $b_{V,profile}$ evaluated by the profile method using this corrected dependence of the coefficients on the velocity of phases depend neither on the reboiler duty nor on the distillation system and are specific only for the model (RBF, BS, or DELFT). Correlations of k_La and k_Va coefficients with the improved flow dependence according to the profile method are presented in the form of eqs 36, 37 and 38. HETP values calculated according to the three suggested correlations practically coincide, with the differences between them reaching 8% at most.

The experimental concentration profiles differ from the profiles calculated from the *Aspen Plus* simulation program. The differences reach up to 70% for the RBF model and 1800% for the BS model. The profile method correlation (36) fits the profiles accurately.

The profile method allows evaluation of the volumetric mass-transfer coefficients in the individual phases in distillation columns, in a manner similar to that also possible in absorption columns, and thereby substantial improvement to the mass-transfer models of distillation and to their validation.

Appendix

A full list of the source data is given in Tables A1−A3 for the distillation systems M−E, E−P, and M−P, respectively.

Nomenclature

a = effective mass-transfer area, m^{-1}
a_p = packing geometrical area, m^{-1}
B = superficial liquid velocity, m h^{-1}
b = triangular channel base dimension, m^{-1}
$b_{L,V}$ = empirical correction factors obtained by using eq 25 in the profile method
$b_{L,V,profile}$ = empirical correction factors obtained by using eq 35 in the profile method
$b_{L,V,orig}$ = multiplication parameters used in the original models RBF, BS, and DELFT
C_V, C_L = packing-specific constant for the BS model
c = molar concentration, mol m^{-3}
c_p = molar heat, kJ $kmol^{-1}$ K^{-1}
D = diffusion coefficient, m^2 s^{-1}
d_h = equivalent hydraulic diameter defined in eq 8, m
d_{hV} = packing characteristic dimension, eq 12, m
d_s = side dimension of packing corrugation, m
HETP = height equivalent to a theoretical plate, m
F = volumetric flow rate of reflux, L min^{-1}
$F_V = u_V\sqrt{(\rho_V)}$ = gas capacity factor, $Pa^{1/2}$
F_{SE} = surface enhancement factor
g = gravity acceleration, m s^{-2}
h = triangular channel height, m
h_{pe} = height of the packing element, m
h = molar enthalpy, kJ $kmol^{-1}$
h_{LB} = liquid holdup given by eqs 11 and 12 in ref 4
h_{LR} = liquid holdup given by eq 19 in ref 3
Δh_{mix} = heat of mixing, kJ $kmol^{-1}$
Δh_{vap} = molar heat of vaporization, kJ $kmol^{-1}$
K_V = overall mass-transfer coefficient, m s^{-1}
K_A = equilibrium coefficient in the equation $y_A = K_A\, x_A$
k_L = liquid-side mass-transfer coefficient on a more volatile component concentration, m s^{-1}
k_V = vapor-side mass-transfer coefficient on a more volatile component concentration, m s^{-1}
k_La = liquid-side volumetric mass-transfer coefficient, s^{-1}
k_Va = vapor-side volumetric mass-transfer coefficient, s^{-1}
$l_{V,pe}$ = length of the gas flow channel in a packing element, m
L = liquid-phase molar flow, kmol s^{-1}
$m_A = dc^*_{AV}/dc^*_{AL}$ = local slope of equilibrium curve
n_D = refractive index
N = molar flux transferred per unit height of packing, kmol m^{-1} s^{-1}
p = atmospheric pressure, Torr
P = reboiler duty, kW
r = quantity defined by eq 23
R_{liquid} = relative liquid-phase mass-transfer resistance defined by eq 1
Re_{Vrv} = Reynolds number defined by eq 18
s = objective function defined by eq 28
S = column cross section, m^2
$Sc_i = \mu_i/\rho_i\, D_i$ = Schmidt number (i = V, L)

Table A1. Source Experimental Data System M−E

	series 1			series 2			series 3			series 4			series 5			series 6			series 7			series 8		
	P = 30 kW, F = 2.221 L min^{-1}, p = 739 Torr			P = 20 kW, F = 1.415 L min^{-1}, p = 739 Torr			P = 40 kW, F = 3.039 L min^{-1}, p = 739 Torr			P = 10 kW, F = 0.611 L min^{-1}, p = 739 Torr			P = 20 kW, F = 1.398 L min^{-1}, p = 751 Torr			P = 40 kW, F = 3.028 L min^{-1}, p = 751 Torr			P = 30 kW, F = 2.199 L min^{-1}, p = 751 Torr			P = 10 kW, F = 0.622 L min^{-1}, p = 751 Torr		
z, m	t_{sat}, °C	x_A/y_A	t_{exp}, °C	t_{sat}, °C	x_A/y_A	t_{exp}, °C	t_{sat}, °C	x_A/y_A	t_{exp}, °C	t_{sat}, °C	x_A/y_A	t_{exp}, °C	t_{sat}, °C	x_A/y_A	t_{exp}, °C	t_{sat}, °C	x_A/y_A	t_{exp}, °C	t_{sat}, °C	x_A/y_A	t_{exp}, °C	t_{sat}, °C	x_A/y_A	t_{exp}, °C
									Liquid															
0.00	64.88	0.9085		64.76	0.9191		64.90	0.9066		64.64	0.9651		64.86	0.9453		64.95	0.9375		64.94	0.9384		64.69	0.9606	
0.15	65.13	0.8869	65.81	65.02	0.8965	65.67	65.12	0.8876	65.71	64.77	0.9532	65.42	65.04	0.9295	65.81	65.10	0.9249	65.81	65.12	0.9231	65.81	64.85	0.9464	65.62
0.45	65.88	0.8237	66.31	65.71	0.8384	66.07	65.83	0.8281	66.27	65.13	0.9221	65.40	65.52	0.8888	65.93	65.60	0.8819	66.02	65.64	0.8784	66.12	65.25	0.9117	65.64
0.75	66.85	0.7451	67.36	66.62	0.7633	66.97	66.69	0.7576	67.12	65.75	0.8693	66.10	66.19	0.8325	66.64	66.21	0.8303	66.73	66.36	0.8185	66.83	65.94	0.8530	66.39
1.08	67.86	0.6656	68.12	67.71	0.6775	67.88	67.88	0.6642	68.11	66.63	0.7957	66.72	67.01	0.7651	67.24	67.08	0.7597	67.40	67.10	0.7579	67.40	66.85	0.7780	67.21
1.39	69.21	0.5631	69.69	68.99	0.5798	69.74	69.36	0.5523	69.93	67.90	0.6942	68.53	67.96	0.6893	68.82	68.25	0.6673	68.96	68.19	0.6717	68.92	68.31	0.6626	69.16
1.69	71.06	0.4296	71.65	70.73	0.4532	71.36	71.22	0.4187	71.79	69.19	0.5952	69.81	69.48	0.5739	70.25	69.91	0.5420	70.68	69.83	0.5474	70.58	69.65	0.5610	70.44
1.99	72.79	0.3098	73.46	72.53	0.3280	73.08	72.79	0.3101	73.38	71.40	0.4342	72.35	71.31	0.4408	72.21	71.52	0.4263	72.40	71.58	0.4217	72.40	71.88	0.4006	72.88
2.10																								
									Vapor															
0.00																								
0.18	65.90	0.8918	65.83	65.70	0.9026	65.61	65.87	0.8933	65.8	65.09	0.9570	65.03	65.52	0.9341	65.59	65.65	0.9274	65.71	65.67	0.9263	65.72	65.18	0.9523	65.23
0.48	66.86	0.8377	66.78	66.69	0.8472	66.59	66.88	0.8364	66.81	65.69	0.9251	65.62	66.25	0.8951	66.29	66.40	0.8867	66.44	66.38	0.8876	66.45	65.87	0.9154	65.91
0.78	67.89	0.7764	67.82	67.73	0.7859	67.63	67.96	0.7721	67.87	66.48	0.8822	66.3	67.01	0.8522	67.04	67.19	0.8420	67.25	67.17	0.8433	67.19	66.65	0.8724	66.69
1.11	69.29	0.6874	69.21	69.10	0.6999	68.94	69.31	0.6860	69.23	67.54	0.8217	67.3	68.13	0.7861	68.14	68.30	0.7762	68.36	68.35	0.7731	68.38	67.90	0.8002	67.74
1.42	70.91	0.5754	70.81	70.75	0.5872	70.64	71.00	0.5691	70.93	69.19	0.7201	68.98	69.66	0.6896	69.62	69.79	0.6808	69.89	69.76	0.6827	69.83	69.62	0.6920	69.45
1.72	72.53	0.4535	72.51	72.38	0.4658	72.28	72.64	0.4447	72.64	70.52	0.6316	70.32	71.11	0.5899	71.15	71.40	0.5691	71.52	71.39	0.5700	71.49	71.11	0.5905	70.98
2.02	74.01	0.3329	74.01	73.89	0.3428	73.84	74.01	0.3333	74.08	72.80	0.4645	72.77	72.86	0.4594	72.97	73.00	0.4483	73.15	73.02	0.4473	73.14	73.14	0.4372	73.21
2.10		0.2624			0.2617			0.2494			0.4243			0.3564			0.3466			0.3449			0.3935	

	series 9			series 10			series 11			series 12			series 13			series 14			series 15			series 16		
	P = 30 kW, F = 2.433 L min^{-1}, p = 744 Torr			P = 40 kW, F = 3.379 L min^{-1}, p = 744 Torr			P = 20 kW, F = 1.543 L min^{-1}, p = 744 Torr			P = 30 kW, F = 2.467 L min^{-1}, p = 744 Torr			P = 20 kW, F = 1.588 L min^{-1}, p = 747 Torr			P = 40 kW, F = 3.463 L min^{-1}, p = 747 Torr			P = 10 kW, F = 0.675 L min^{-1}, p = 747 Torr			P = 10 kW, F = 0.659 L min^{-1}, p = 747 Torr		
z, m	t_{sat}, °C	x_A/y_A	t_{exp}, °C	t_{sat}, °C	x_A/y_A	t_{exp}, °C	t_{sat}, °C	x_A/y_A	t_{exp}, °C	t_{sat}, °C	x_A/y_A	t_{exp}, °C	t_{sat}, °C	x_A/y_A	t_{exp}, °C	t_{sat}, °C	x_A/y_A	t_{exp}, °C	t_{sat}, °C	x_A/y_A	t_{exp}, °C	t_{sat}, °C	x_A/y_A	t_{exp}, °C
									Liquid															
0.00	69.35	0.5655		69.38	0.5637		68.95	0.5954		70.13	0.5083		70.34	0.5005		70.72	0.4729		68.24	0.6573		69.32	0.5754	
0.15	70.18	0.5049	70.97	70.14	0.5077	70.92	69.97	0.5201	70.82	70.99	0.4470	71.75	71.43	0.4230	72.43	71.53	0.4157	72.43	69.38	0.5709	70.24	70.70	0.4748	71.60
0.45	72.21	0.3616	72.65	72.00	0.3757	72.41	71.95	0.3795	72.31	72.98	0.3091	73.33	73.32	0.2925	73.71	73.35	0.2910	73.81	71.47	0.4200	71.88	72.74	0.3319	73.08
0.75	73.75	0.2573	74.23	73.52	0.2724	73.99	73.56	0.2698	73.89	74.44	0.2113	74.71	74.69	0.2021	75.10	74.69	0.2021	75.10	73.60	0.2742	73.94	74.60	0.2079	74.90
1.08	74.84	0.1855	75.05	74.86	0.1843	75.03	74.77	0.1898	74.91	75.36	0.1518	75.49	75.63	0.1406	75.80	75.75	0.1330	75.97	74.76	0.1971	75.01	75.53	0.1474	75.70
1.39	75.76	0.1262	76.07	75.90	0.1169	76.21	75.55	0.1394	75.82	76.16	0.1003	76.40	76.26	0.1007	76.55	76.56	0.0818	76.84	76.13	0.1088	76.40	76.57	0.0810	76.79
1.69	76.61	0.0723	76.77	76.66	0.0689	76.87	76.43	0.0834	76.63	76.86	0.0564	76.96	76.91	0.0597	77.21	77.11	0.0472	77.35	76.70	0.0727	76.87	77.01	0.0535	77.21
1.99	77.04	0.0446	77.23	77.08	0.0425	77.28	76.96	0.0497	77.09	77.23	0.0332	77.33	77.30	0.0353	77.57	77.40	0.0285	77.62	77.15	0.0442	77.43	77.40	0.0289	77.57
2.10																								
									Vapor															
0.00																								
0.18	71.96	0.5108	71.89	71.80	0.5226	71.72	71.58	0.5392	71.44	72.74	0.4506	72.60	72.94	0.4428	72.96	73.09	0.4306	73.11	70.89	0.5960	70.77	72.06	0.5108	71.96
0.48	73.48	0.3911	73.48	73.54	0.3867	73.47	73.34	0.4023	73.21	74.18	0.3326	74.10	74.49	0.3152	74.52	74.66	0.3008	74.68	73.08	0.4313	72.94	74.11	0.3473	74.03
0.78	74.66	0.2918	74.6	74.73	0.2856	74.64	74.48	0.3073	74.36	75.20	0.2438	75.12	75.44	0.2322	75.48	75.65	0.2128	75.67	74.51	0.3134	74.42	75.29	0.2450	75.23
1.11	75.67	0.2014	75.62	75.72	0.1971	75.65	75.53	0.2144	75.39	76.07	0.1648	76.00	76.24	0.1585	76.26	76.40	0.1430	76.45	75.70	0.2086	75.51	76.26	0.1569	76.11
1.42	76.43	0.1310	76.39	76.50	0.1246	76.45	76.35	0.1387	76.22	76.72	0.1035	76.63	76.82	0.1035	76.87	76.97	0.0888	77.02	76.56	0.1278	76.44	76.91	0.0945	76.82
1.72	76.95	0.0805	76.96	77.02	0.0743	77.03	76.87	0.0884	76.82	77.13	0.0627	77.10	77.24	0.0623	77.31	77.36	0.0501	77.46	77.05	0.0810	77.00	77.27	0.0597	77.22
2.02	77.29	0.0472	77.33	77.29	0.0472	77.36	77.24	0.0522	77.20	77.41	0.0353	77.39	77.51	0.0357	77.60	77.56	0.0302	77.70	77.41	0.0455	77.41	77.55	0.0315	77.53
2.10		0.0306			0.0281			0.0353			0.0217			0.0247			0.0191			0.0366			0.0268	

Table A2. Source Experimental Data System E−P

	series 1			series 2			series 3			series 4			series 5			series 6			series 7			series 8		
	P = 40 kW, F = 3.955 L min^{-1}, p = 749 Torr			P = 30 kW, F = 2.86 L min^{-1}, p = 749 Torr			P = 20 kW, F = 1.82 L min^{-1}, p = 749 Torr			P = 10 kW, F = 0.81 L min^{-1}, p = 749 Torr			P = 40 kW, F = 3.98 L min^{-1}, p = 749 Torr			P = 30 kW, F = 2.87 L min^{-1}, p = 749 Torr			P = 20 kW, F = 1.8 L min^{-1}, p = 745 Torr			P = 10 kW, F = 0.795 L min^{-1} p = 745 Torr		
z, m	t_{sat}, °C	x_A/ y_A	t_{exp}, °C	t_{sat}, °C	x_A/ y_A	t_{exp}, °C	t_{sat}, °C	x_A/ y_A	t_{exp}, °C	t_{sat}, °C	x_A/ y_A	t_{exp}, °C	t_{sat}, °C	x_A/ y_A	t_{exp}, °C	t_{sat}, °C	x_A/ y_A	t_{exp}, °C	t_{sat}, °C	x_A/ y_A	t_{exp}, °C	t_{sat}, °C	x_A/ y_A	t_{exp}, °C
												Liquid												
0.00	79.05	0.9113		79.09	0.9085		78.94	0.9199		78.44	0.9592		81.19	0.7542		81.21	0.7527		80.48	0.7947		79.96	0.8325	
0.15	79.38	0.8862	79.64	79.51	0.8767	79.71	79.33	0.8901	79.55	78.82	0.9292	79.10	81.89	0.7064	82.24	82.09	0.6929	82.36	81.28	0.7388	81.60	81.11	0.7505	81.92
0.45	80.50	0.8035	80.94	80.66	0.7921	81.17	80.55	0.7995	80.99	79.46	0.8806	79.68	84.09	0.5652	84.87	84.42	0.5454	85.15	83.57	0.5890	84.18	83.02	0.6229	83.68
0.75	81.77	0.7141	82.53	82.14	0.6891	83.09	82.14	0.6894	82.95	80.83	0.7799	81.42	86.40	0.4330	87.65	87.00	0.4012	88.33	86.03	0.4457	87.17	85.98	0.4488	87.50
1.08	83.81	0.5824	85.15	84.35	0.5495	85.65	84.13	0.5632	85.44	82.59	0.6598	83.90	89.32	0.2870	90.86	89.67	0.2705	91.09	88.38	0.3251	89.91	89.05	0.2931	90.96
1.39	86.63	0.4207	88.05	86.63	0.4211	88.05	85.96	0.4574	87.26	85.24	0.4974	87.02	92.12	0.1652	93.26	91.95	0.1721	93.15	90.28	0.2372	91.45	91.63	0.1795	93.13
1.69	89.55	0.2762	90.98	89.99	0.2563	91.41	89.51	0.2781	90.97	88.34	0.3338	89.88	94.00	0.0919	94.92	94.15	0.0863	95.05	93.06	0.1223	94.17	93.79	0.0945	94.76
1.99	92.21	0.1612	93.40	92.23	0.1607	93.50	92.04	0.1682	93.33	91.71	0.1819	93.17	95.17	0.0492	95.93	95.17	0.0492	95.87	94.49	0.0689	95.35	95.17	0.0446	95.87
2.10																								
												Vapor												
0.00																								
0.18	80.44	0.8943	80.82	80.63	0.8862	80.99	80.40	0.8960	80.69	79.33	0.9415	79.49	84.18	0.7252	84.34	84.61	0.7045	84.66	83.37	0.7569	83.47	82.51	0.7965	82.63
0.48	82.13	0.8202	82.68	82.25	0.8144	82.77	82.01	0.8253	82.475	80.54	0.8901	80.83	87.00	0.5853	87.42	87.21	0.5743	87.61	85.98	0.6305	86.33	85.49	0.6551	85.9
0.78	83.94	0.7365	84.53	84.09	0.7297	84.61	83.90	0.7384	84.41	82.10	0.8213	82.48	89.47	0.4522	89.94	89.55	0.4479	89.94	88.32	0.5080	88.71	88.20	0.5144	88.66
1.11	86.57	0.6076	87.31	86.69	0.6011	87.36	86.62	0.6048	87.215	84.61	0.7049	84.96	91.98	0.3052	92.61	91.87	0.3122	92.48	90.90	0.3621	91.39	91.26	0.3403	91.66
1.42	89.56	0.4470	90.34	89.71	0.4387	90.45	89.51	0.4501	90.19	88.18	0.5232	88.81	93.93	0.1829	94.61	93.95	0.1814	94.58	92.99	0.2339	93.65	93.64	0.1927	94.24
1.72	92.26	0.2884	92.91	92.09	0.2987	92.71	91.84	0.3140	92.38	90.81	0.3752	91.34	95.29	0.0919	95.82	95.11	0.1041	95.61	94.44	0.1398	94.92	94.84	0.1132	95.32
2.02	94.14	0.1691	94.81	94.11	0.1711	94.69	93.99	0.1790	94.53	93.53	0.2088	94.04	95.92	0.0492	96.56	95.88	0.0518	96.43	95.48	0.0699	96.03	95.69	0.0555	96.24
2.10		0.1056			0.1208			0.1288			0.1746			0.0295			0.0347			0.0425			0.0446	

	series 1			series 2			series 3			series 4			series 5			series 6			series 7			series 8		
	P = 40 kW, F = 4.23 L min^{-1}, p = 745 Torr			P = 30 kW, F = 3.045 L min^{-1}, p = 745 Torr			P = 20 kW, F = 1.92 L min^{-1}, p = 745 Torr			P = 10 kW, F = 0.835 L min^{-1}, p = 745 Torr			P = 20 kW, F = 1.79 L min^{-1}, p = 756 Torr			P = 10 kW, F = 0.795 L min^{-1}, p = 756 Torr			P = 40 kW, F = 3.91 L min^{-1}, p = 756 Torr			P = 30 kW, F = 2.82 L min^{-1}, p = 757 Torr		
z, m	t_{sat}, °C	x_A/ y_A	t_{exp}, °C	t_{sat}, °C	x_A/ y_A	t_{exp}, °C	t_{sat}, °C	x_A/ y_A	t_{exp}, °C	t_{sat}, °C	x_A/ y_A	t_{exp}, °C	t_{sat}, °C	x_A/ y_A	t_{exp}, °C	t_{sat}, °C	x_A/ y_A	t_{exp}, °C	t_{sat}, °C	x_A/ y_A	t_{exp}, °C	t_{sat}, °C	x_A/ y_A	t_{exp}, °C
												Liquid												
0.00	84.67	0.5224		84.59	0.5274		84.35	0.5416		82.80	0.6373		79.22	0.9168		78.85	0.9453		79.31	0.9099		79.39	0.9061	
0.15	85.92	0.4518	87.06	85.92	0.4518	87.04	85.88	0.4540	87.05	85.15	0.4948	86.82	79.53	0.8925	79.67	79.18	0.9196	79.45	79.60	0.8873	79.79	79.72	0.8809	79.85
0.45	89.13	0.2893	90.43	89.21	0.2856	90.47	89.49	0.2724	90.51	88.13	0.3371	89.30	80.51	0.8195	80.80	79.80	0.8721	79.96	80.51	0.8195	80.92	80.72	0.8068	81.09
0.75	91.50	0.1849	92.83	91.82	0.1716	93.02	91.81	0.1721	92.95	91.44	0.1873	92.68	81.87	0.7236	82.53	81.07	0.7792	81.65	81.65	0.7388	82.33	82.02	0.7160	82.84
1.08	93.59	0.1021	94.86	93.57	0.1026	94.76	93.40	0.1092	94.61	93.28	0.1137	94.66	83.44	0.6201	84.58	82.87	0.6570	84.09	83.48	0.6177	84.69	83.94	0.5910	85.13
1.39	94.98	0.0513	95.75	94.82	0.0570	95.61	94.36	0.0735	95.25	94.56	0.0663	95.46	85.17	0.5156	86.40	85.35	0.5050	87.18	86.11	0.4622	87.51	86.15	0.4618	87.51
1.69	95.71	0.0258	96.38	95.72	0.0253	96.34	95.56	0.0310	96.21	95.45	0.0347	96.13	88.61	0.3325	90.18	88.36	0.3444	90.06	89.02	0.3126	90.59	89.42	0.2949	90.96
1.99	96.10	0.0127	96.67	96.05	0.0143	96.59	95.97	0.0169	96.53	95.94	0.0179	96.48	91.23	0.2122	92.72	91.90	0.1839	93.43	91.58	0.1976	93.14	91.83	0.1883	93.25
2.10																								
												Vapor												
0.00																								
0.18	88.79	0.4825	89.39	89.00	0.4708	89.59	88.91	0.4756	89.42	87.26	0.5648	87.81	80.55	0.8998	80.61	79.80	0.9316	79.8	80.65	0.8953	80.85	80.87	0.8873	80.99
0.48	91.69	0.3149	92.49	91.80	0.3080	92.43	91.59	0.3209	92.24	90.68	0.3748	91.35	81.90	0.8408	82.14	80.93	0.8834	81.1	82.10	0.8318	82.49	82.27	0.8257	82.6
0.78	93.63	0.1932	94.23	93.49	0.2025	94.03	93.28	0.2155	93.84	92.74	0.2496	93.34	83.46	0.7699	83.83	82.38	0.8192	82.69	83.71	0.7587	84.17	83.88	0.7520	84.28
1.11	94.94	0.1066	95.56	94.79	0.1163	95.38	94.65	0.1258	95.275	94.40	0.1428	94.96	85.86	0.6551	86.39	84.79	0.7072	85.15	86.18	0.6392	86.81	86.33	0.6333	86.86
1.42	95.66	0.0575	96.39	95.56	0.0642	96.27	95.49	0.0689	96.17	95.39	0.0761	96.09	88.64	0.5110	89.34	88.27	0.5307	88.93	89.03	0.4897	89.91	89.22	0.4812	89.99
1.72	96.13	0.0242	96.73	96.03	0.0316	96.58	95.96	0.0363	96.48	95.84	0.0446	96.38	91.11	0.3721	91.70	90.92	0.3829	91.50	91.81	0.3302	92.56	91.70	0.3389	92.41
2.02	96.32	0.0111	96.99	96.27	0.0143	96.90	96.24	0.0164	96.86	96.15	0.0232	96.75	93.59	0.2204	94.25	93.65	0.2165	94.29	93.92	0.1990	94.68	93.92	0.2015	94.60
2.10		0.0058			0.0090			0.0085			0.0200			0.1667			0.1805			0.1298			0.1363	

Table A3. Source Experimental Data System M−P

	series 1 (P = 20 kW, F = 1.43 L min^{-1}, p = 745 Torr)			series 3 (P = 40 kW, F = 2.99 L min^{-1}, p = 746 Torr)			series 8 (P = 30 kW, F = 2.16 L min^{-1}, p = 746 Torr)			series 9 (P = 40 kW, F = 2.98 L min^{-1}, p = 746 Torr)			series 12 (P = 20 kW, F = 1.38 L min^{-1}, p = 746 Torr)			series 13 (P = 30 kW, F = 2.15 L min^{-1}, p = 746 Torr)			series 14 (P = 20 kW, F = 1.37 L min^{-1}, p = 746 Torr)			series 15 (P = 40 kW, F = 2.97 L min^{-1} p = 746 Torr)		
z, m	t_{sat}, °C	x_A/ y_A	t_{exp}, °C	t_{sat}, °C	x_A/ y_A	t_{exp}, °C	t_{sat}, °C	x_A/ y_A	t_{exp}, °C	t_{sat}, °C	x_A/ y_A	t_{exp}, °C	t_{sat}, °C	x_A/ y_A	t_{exp}, °C	t_{sat}, °C	x_A/ y_A	t_{exp}, °C	t_{sat}, °C	x_A/ y_A	t_{exp}, °C	t_{sat}, °C	x_A/ y_A	t_{exp}, °C
Liquid																								
0.00	67.44	0.8028		65.12	0.9320		64.47	0.9744		64.66	0.9615		64.36	0.9814		64.75	0.9557		64.60	0.9657		64.45	0.9757	
0.15	70.54	0.6728	72.43	65.49	0.9091	66.18	64.68	0.9603	65.05	64.91	0.9453	65.44	64.60	0.9656	65.17	65.09	0.9337	65.65	64.97	0.9417	65.86	64.62	0.9644	64.88
0.45	78.94	0.4045	80.19	67.79	0.7880	69.06	65.54	0.9058	66.32	66.15	0.8706	67.26	65.32	0.9193	65.98	66.77	0.8374	68.10	66.27	0.8639	67.34	65.35	0.9176	65.97
0.75	87.45	0.1903	88.48	71.86	0.6258	74.16	67.50	0.8015	69.26	68.71	0.7475	70.67	67.21	0.8156	68.91	70.32	0.6824	72.61	69.54	0.7130	71.81	66.89	0.8317	68.19
1.08	91.84	0.0938	93.05	79.19	0.3987	81.26	71.66	0.6328	73.51	74.14	0.5491	76.54	71.19	0.6500	74.33	76.47	0.4768	78.71	75.80	0.4968	78.62	70.31	0.6830	72.45
1.39	93.75	0.0542	94.50	87.84	0.1822	89.13	78.37	0.4215	80.60	82.68	0.3063	84.51	77.58	0.4442	80.57	84.26	0.2667	85.80	82.82	0.3027	84.59	77.47	0.4473	79.76
1.69	95.95	0.0101	96.45	93.14	0.0673	93.84	88.04	0.1776	89.53	90.57	0.1216	91.55	88.26	0.1726	89.67	91.86	0.0940	92.75	91.54	0.1009	92.37	86.78	0.2065	88.13
1.99	96.22	0.0050	96.67	95.32	0.0234	95.87	92.83	0.0737	93.86	94.19	0.0460	95.00	92.93	0.0717	93.98	94.63	0.0371	95.25	94.54	0.0389	95.17	92.30	0.0849	93.24
2.10																								
Vapor																								
0.00																								
0.18	77.86	0.7416	77.24	68.89	0.9205	69.02	66.03	0.9657	66.29	67.05	0.9507	67.27	65.53	0.9733	65.90	67.69	0.9410	67.72	66.76	0.9549	66.92	65.85	0.9684	66.05
0.48	86.38	0.4758	85.60	73.93	0.8175	74.62	68.69	0.9257	68.65	70.90	0.8893	70.57	68.26	0.9324	68.29	71.98	0.8699	71.47	71.12	0.8855	70.65	68.46	0.9292	68.32
0.78	91.25	0.2711	90.93	79.50	0.6787	80.24	72.88	0.8529	72.65	75.80	0.7915	75.43	72.40	0.8620	72.07	77.32	0.7557	76.66	76.35	0.7789	75.58	72.33	0.8633	72.06
1.11	94.44	0.1124	94.54	86.39	0.4533	87.00	79.52	0.6989	78.70	82.29	0.6178	81.66	79.32	0.7043	78.58	84.39	0.5487	83.41	83.85	0.5671	82.75	78.06	0.7372	77.44
1.42	95.74	0.0416	96.20	92.21	0.2151	92.46	87.05	0.4514	86.54	89.54	0.3492	89.17	87.07	0.4506	86.54	90.90	0.2888	90.42	90.73	0.2965	90.11	85.81	0.4984	85.20
1.72	96.22	0.0147	96.65	95.59	0.0766	95.14	92.19	0.2281	92.23	93.80	0.1478	93.84	92.02	0.2365	91.84	94.18	0.1280	94.17	93.94	0.1404	93.74	91.53	0.2595	91.36
2.02	96.39	0.0047	96.93	97.00	0.0231	96.11	95.13	0.0772	95.45	95.71	0.0454	96.18	95.18	0.0743	95.47	95.80	0.0401	96.15	95.77	0.0422	96.10	94.88	0.0906	95.07
2.10		0.0029			0.0068			0.0386			0.0195			0.0368			0.0192			0.0216			0.0469	

	series 17 (P = 30 kW, F = 2.17 L min^{-1}, p = 746 Torr)			series 18 (P = 40 kW, F = 3.00 L min^{-1}, p = 746 Torr)			series 20 (P = 30 kW, F = 2.16 L min^{-1}, p = 748 Torr)			series 21 (P = 20 kW, F = 1.37 L min^{-1}, p = 748 Torr)			series 22 (P = 10 kW, F = 0.605 L min^{-1}, p = 748 Torr)			series 23 (P = 10 kW, F = 0.603 L min^{-1}, p = 746 Torr)			series 24 (P = 10 kW, F = 0.603 L min^{-1}, p = 746 Torr)			series 25 (P = 10 kW, F = 0.603 L min^{-1}, p = 746 Torr)		
z, m	t_{sat}, °C	x_A/ y_A	t_{exp}, °C	t_{sat}, °C	x_A/ y_A	t_{exp}, °C	t_{sat}, °C	x_A/ y_A	t_{exp}, °C	t_{sat}, °C	x_A/ y_A	t_{exp}, °C	t_{sat}, °C	x_A/ y_A	t_{exp}, °C	t_{sat}, °C	x_A/ y_A	t_{exp}, °C	t_{sat}, °C	x_A/ y_A	t_{exp}, °C	t_{sat}, °C	x_A/ y_A	t_{exp}, °C
Liquid																								
0.00	64.56	0.9684		64.62	0.9645		64.79	0.9578		64.61	0.9698		64.31	0.9893		64.58	0.9667		64.56	0.9685		64.39	0.9797	
0.15	64.80	0.9526	65.16	64.85	0.9491	65.22	65.10	0.9378	65.65	64.99	0.9446	65.83	64.50	0.9765	64.96	65.24	0.9241	66.39	65.16	0.9292	66.26	64.76	0.9555	65.50
0.45	65.92	0.8835	66.84	65.96	0.8814	66.88	66.62	0.8487	67.85	66.16	0.8738	67.20	65.02	0.9425	65.55	67.04	0.8238	68.61	66.94	0.8291	68.54	65.82	0.8892	66.98
0.75	68.49	0.7570	70.28	68.20	0.7694	69.98	70.12	0.6927	72.14	69.38	0.7222	71.57	67.14	0.8227	68.93	73.27	0.5775	75.66	72.98	0.5871	75.51	69.92	0.6982	72.51
1.08	73.46	0.5710	75.73	73.07	0.5842	75.53	76.12	0.4892	77.83	75.21	0.5173	78.35	73.15	0.5838	76.49	83.44	0.2871	85.65	83.01	0.2977	85.17	78.84	0.4084	81.70
1.39	80.99	0.3499	82.99	81.80	0.3288	83.51	83.65	0.2835	84.56	81.82	0.3299	83.31	83.51	0.2871	85.29	90.65	0.1199	91.85	89.94	0.1352	91.43	88.45	0.1683	89.58
1.69	90.01	0.1338	91.12	89.89	0.1363	90.78	91.66	0.0997	92.49	91.23	0.1090	92.02	91.40	0.1054	91.71	94.84	0.0330	95.22	94.79	0.0338	95.13	93.93	0.0513	94.17
1.99	93.81	0.0536	94.51	93.84	0.0530	94.53	94.58	0.0395	95.22	94.43	0.0424	95.11	94.95	0.0321	95.38	95.91	0.0117	96.36	95.97	0.0105	96.37	95.68	0.0162	96.06
2.10																								
Vapor																								
0.00																								
0.18	66.57	0.9578	66.72	66.75	0.9551	66.90	67.50	0.9449	67.62	66.68	0.9571	66.87	64.97	0.9835	65.26	67.25	0.9477	67.52	66.99	0.9516	67.36	65.85	0.9685	66.24
0.48	70.07	0.9035	69.71	70.44	0.8972	70.05	71.43	0.8810	71.08	70.72	0.8935	70.37	67.34	0.9473	67.46	73.72	0.8362	72.86	73.36	0.8435	72.60	70.45	0.8971	70.09
0.78	74.79	0.8139	74.26	75.21	0.8047	74.71	76.76	0.7708	76.28	75.81	0.7928	75.16	71.83	0.8738	71.68	80.95	0.6583	79.65	80.45	0.6727	79.22	76.84	0.7674	76.06
1.11	81.79	0.6330	80.80	81.64	0.6377	80.83	83.74	0.5729	82.81	83.19	0.5911	82.23	79.80	0.6929	78.75	88.93	0.3755	87.66	88.94	0.3750	87.46	85.90	0.4951	84.21
1.42	88.98	0.3733	88.36	88.86	0.3784	88.21	90.38	0.3152	89.94	90.07	0.3293	89.50	89.28	0.3632	88.43	94.27	0.1233	94.03	94.17	0.1285	93.87	92.88	0.1943	92.36
1.72	93.23	0.1768	93.06	93.44	0.1659	93.26	93.92	0.1453	93.92	93.60	0.1616	93.44	93.36	0.1736	92.99	95.64	0.0489	95.75	95.61	0.0510	95.71	94.97	0.0858	94.87
2.02	95.50	0.0569	95.72	95.56	0.0536	95.83	95.79	0.0448	96.16	95.79	0.0445	96.09	95.74	0.0478	95.96	96.24	0.0153	96.70	96.27	0.0138	96.70	96.11	0.0231	96.48
2.10		0.0324			0.0264			0.0234			0.0228			0.0350			0.0108			0.0098			0.0165	

Series 2, 4−7, 10, 11, and 16 were not utilized for evaluation because molar fractions of one of components reached values higher than 0.99 at the top or bottom of the column.

$Sh_{V,i}$ = Sherwood number (i = turd, lam) defined by eq 16 or 17
t = temperature, °C
u = superficial velocity, m s^{-1}
u_{LE} = average liquid velocity in an actual liquid-flow cross section defined by eq 3, m s^{-1}
u_{VE} = average liquid velocity in an actual liquid-flow cross section defined by eq 5, m s^{-1}
x_A = mole fraction of a more volatile component in the liquid phase
y_A = mole fraction of a more volatile component in the vapor phase
z = packing height coordinate taken from the top (z = 0), m

Subscripts

L = liquid phase
V = vapor/gas phase
PM = profile method
profile = profile method
orig = original RBF, BS, or DELFT model
w = vapor−liquid interface

Superscripts

α, β, γ, δ, ε = exponents in relation (29)
λ, υ = exponents in relation (33)
* = equilibrium value

Greek Symbols

α = corrugation angle, deg
δ = liquid film thickness defined by eq 13 or 29, m
ε = packing porosity
φ = fraction of the channel occupied by the liquid defined by eq 19
γ = contact angle, deg
μ = viscosity, Pa s
ρ = density, kg m^{-3}
σ = surface tension, N m^{-1}
ξ_{VL} = friction factor defined by eq 19
Ω = packing surface void fraction

Acknowledgment

Financial support from the Ministry of Education (Grant MSM 6046137306) is gratefully acknowledged.

Literature Cited

(1) Wang, G. Q.; Yuan, X. G.; Yu, K. T. Review of mass-transfer correlations for packed columns. *Ind. Eng. Chem. Res.* **2005**, *44*, 8715.

(2) Rocha, J. A.; Bravo, J. L.; Fair, J. R. Distillation columns containing structured packings: A comprehensive model for their performance. 2. Mass-transfer model. *Ind. Eng. Chem. Res.* **1996**, *35*, 1660.

(3) Rocha, J. A.; Bravo, J. L.; Fair, J. R. Distillation columns containing structured packings: A comprehensive model for their performance. 1. Hydraulic models. *Ind. Eng. Chem. Res.* **1993**, *32*, 641.

(4) Billet, R.; Schultes, M. Prediction of mass transfer columns with dumped and arranged packings. Updated summary of the calculation method of Billet and Schultes. *Trans. Inst. Chem. Eng.* **1999**, *77*, 498.

(5) Olujič, Ž.; Kamerbeek, A. B.; de Graauw, J. A. Corrugation geometry based model for efficiency of structured distillation packing. *Chem. Eng. Proc.* **1999**, *38*, 683.

(6) Taylor, R. (Di)Still modeling after all these years: A view of the state of the art. *Ind. Eng. Chem. Res.* **2007**, *46*, 4349.

(7) Linek, V.; Moucha, T.; Prokopová, E.; Rejl, J. F. Simultaneous determination of vapour- and liquid-side volumetric mass transfer coefficients in distillation column. *Trans. Inst. Chem. Eng., Chem. Eng. Res. Des.* **2005**, *83* (A8), 979.

(8) Rejl, F.; Linek, V.; Moucha, T.; Prokopová, E.; Valenz, L.; Hovorka, F. Vapour- and liquid-side volumetric mass transfer coefficients measured in distillation column. Comparison with data calculated from absorption correlations. *Chem. Eng. Sci.* **2006**, *61*, 6096.

(9) Shi, M. G.; Mersmann, A. Effective interfacial area in packed columns. *Ger. Chem. Eng.* **1985**, *8*, 87.

(10) Onda, K.; Takeuchi, H.; Okumoto, Y. Mass transfer coefficients between gas and liquid phases in packed columns. *J. Chem. Eng. Jpn.* **1968**, *1*, 56.

(11) Vargaftik, N. B. *Tables on the Thermophysical Properties of Liquids and Gases*, 2nd ed.; Wiley: New York, 1975.

(12) Zábranský, M.; Růžička, V.; Majer, V.; Domalski, E. S. Heat Capacities of Liquids, Critical Review and Recommended Values. *Journal of Physical and Chemical Reference Data, Monograph*; American Chemical Society: Washington, DC, 1996; No. 6.

(13) Majer, V.; Svoboda, V. Enthalpies of Vaporization of Organic Compounds. *IUPAC Chemical Data Series No. 32*; Blackwell: Oxford, U.K., 1985.

(14) Yaws, C. L. *Chem. Eng.* **1976**, Oct 25.

(15) Ried, R. C.; Prausnitz, J. M.; Poling, B. E. *The Properties of Gases and Liquids*, 4th ed.; McGraw-Hill Book Company: Singapore, 1988.

(16) Chung, T. H.; Lee, L. L.; Starling, K. E. Applications of Kinetic Gas Theories and Multiparameter Correlation for Prediction of Dilute Gas Viscosity and Thermal Conductivity. *Ind. Eng. Chem. Fundam.* **1984**, *23*, 8.

(17) Gmehling, J.; Onken, N. Vapor−Liquid Equilibrium Data Collection, Alcohols−Supplement 3, Chemistry Data Series. *Dechema, Frakfurt am Main* **1991**, *1*, Part 2e.

(18) Zarzycki, R.; Chacuk, A. *Absorption Fundamentals & Applications*; Pergamon Press: London, 1993; p 42.

(19) Krishna, R.; Wesselingh, J. A. The Maxwell−Stefan approach to mass transfer. *Chem. Eng. Sci.* **1997**, *52*, 861.

(20) Valenz, L. Study of interfacial heat and mass transfer in packed distillation and absorption columns. An effect of axial dispersion in both phases. Dissertation, Prague Institute of Chemical Technology, Prague, Czech Republic, 2009.

(21) Rejl, J. F.; Linek, V.; Moucha, T.; Valenz, L. Methods standardization in the measurement of mass transfer characteristics in packed absorption columns. *Chem. Eng. Res. Des.* **2009**, *87*, 695.

(22) Bravo, J. L.; Rocha, J. A.; Fair, J. R. A comprehensive model for the performance of columns containing structured packings. *Inst. Chem. Eng. Symp. Ser.* **1992**, *128*, A489 Distillation and Absorption ′92, Vol. 1.

(23) Billet, R.; Schultes, M. Predicting mass transfer in packed columns. *Chem. Eng. Technol.* **1993**, *16* (1), 1.

Received for review October 28, 2009
Revised manuscript received February 11, 2010
Accepted March 4, 2010

IE901690M